



UNITED NATIONS EDUCATIONAL, SCIENTIFIC AND CULTURAL ORGANIZATION  
INTERNATIONAL ATOMIC ENERGY AGENCY  
INTERNATIONAL CENTRE FOR THEORETICAL PHYSICS  
I.C.T.P., P.O. BOX 586, 34100 TRIESTE, ITALY, CABLE: CENTRATOM TRIESTE



**SMR.998a - 20**

Research Workshop on Condensed Matter Physics  
30 June - 22 August 1997  
**MINIWORKSHOP ON**  
**QUANTUM MONTE CARLO SIMULATIONS OF LIQUIDS AND SOLIDS**  
30 JUNE - 11 JULY 1997  
and  
**CONFERENCE ON**  
**QUANTUM SOLIDS AND POLARIZED SYSTEMS**  
3 - 5 JULY 1997

---

**"Ground state magnetic order in a  
frustrated two dimensional magnet;  
multiple spin exchange in adsorbed solid  $^3\text{He}$  films"**

**J. SAUNDERS**  
**Royal Holloway**  
**University of London**  
**Department of Physics**  
**Egham Hill**  
**Surrey**  
**TW20 0EX**  
**U.K.**

---

**These are preliminary lecture notes, intended only for distribution to participants.**

MAIN BUILDING STRADA COSTIERA, 11 TEL. 2240111 TELEFAX 224163 TELEX 460392 ADRIATICO GUEST HOUSE VIA GRIGNANO, 9 TEL. 224241 TELEFAX 224531 TELEX 460449  
MICROPROCESSOR LAB. VIA BEIRUT, 31 TEL. 2249911 TELEFAX 224600 TELEX 460392 GALILEO GUEST HOUSE VIA BEIRUT, 7 TEL. 2240311 TELEFAX 2240310 TELEX 460392

# Ground state magnetic order in a frustrated two dimensional magnet; multiple spin exchange in adsorbed solid $^3\text{He}$ films

*Marcio Siqueira (EPSRC student, now at Oxford Instruments)*

*Martin Dann (EPSRC student)*

*Jan Nyéki (EPSRC)*

*Brian Cowan*

*John Saunders*

***Millikelvin Laboratory, Department of Physics, Royal  
Holloway University of London, Egham, TW20 0EX***

1. Frustrated magnets
2. Nuclear magnetic exchange in solid  $^3\text{He}$
3. Helium films

**$\Rightarrow$  model two dimensional magnetic systems**

4. Multiple spin exchange
5. Heat capacity and magnetization measurements to  $T < 1\text{mK}$
6. "Tunable" ground state order
7. Phase transitions

8. Conclusions and the future

*Phys. Rev. Lett.* 78, 2600 ('97)

*Phys. Rev. Lett.* 76, 1584 ('96)

*Czech. J. Phys. Supp* 56 25,  
3033 (1996)

Research supported by EPSRC

[j.saunders@rhbnc.ac.uk](mailto:j.saunders@rhbnc.ac.uk)

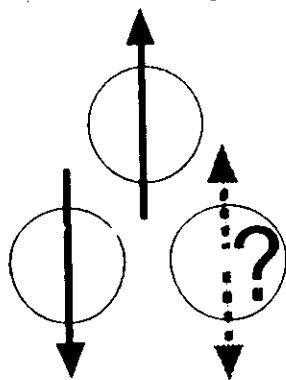
# FRUSTRATED MAGNETS

Consider structurally ordered materials

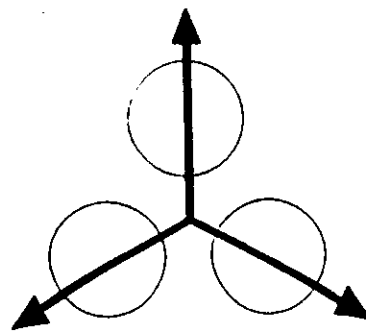
- geometrical frustration
- frustration due to competing exchange interactions

## 1. geometrical frustration in 2D

(i) triangular lattice (potential candidate  $\text{NaTiO}_2$ , Hirakawa, Kawodaki and Ubukoshi, 1985)



(a)

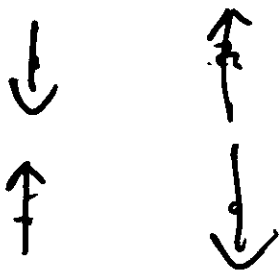


(b)

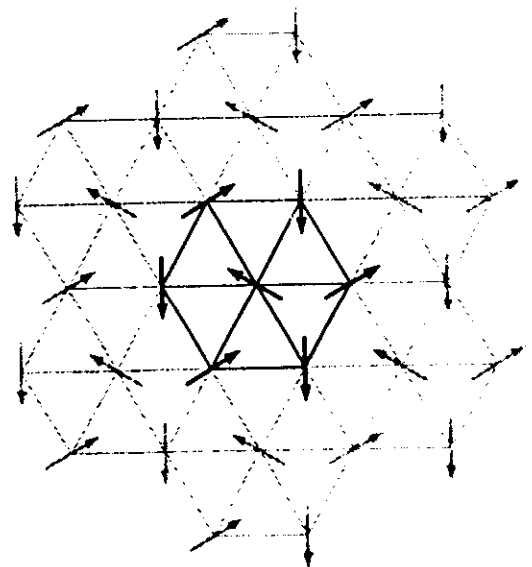
classical  
ground state

$$\mathcal{H} = -J \vec{S}_1 \cdot \vec{S}_2$$

antiferromagnetic exchange



3 sub-lattices



# Nuclear magnetic exchange in solid $^3\text{He}$

1. Nuclear spin  $S = 1/2$

2. Heisenberg Hamiltonian  $\mathcal{H} = -J \mathbf{S}_1 \cdot \mathbf{S}_2$

- $J$  is of order mK, much larger than other nuclear magnets
- isotropic interaction

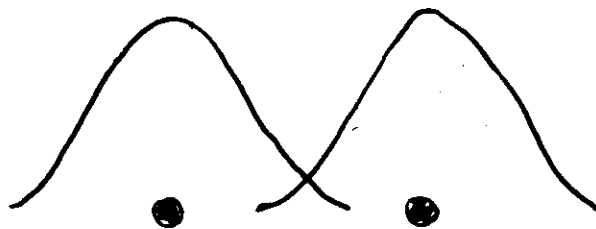
What is physical origin of exchange ?

$^3\text{He}$  is a quantum solid

overlap of atomic wavefunctions due to zero point motion

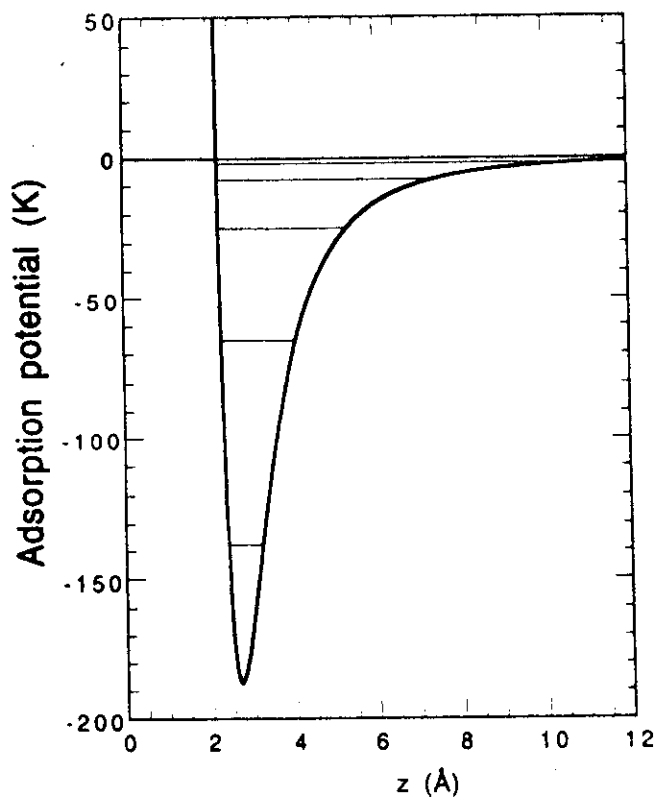
atoms (occasionally) move between sites in crystal

leads to an effective spin - spin interaction of the Heisenberg form

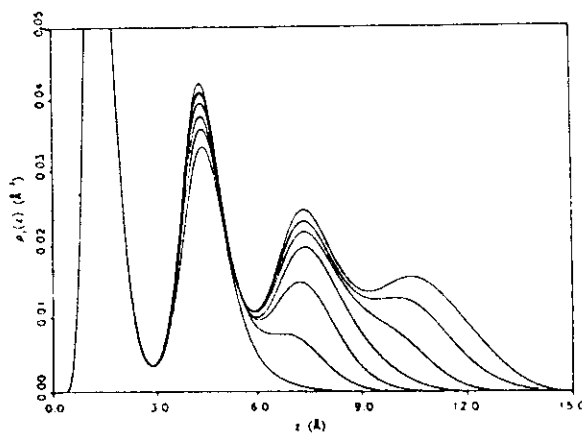


## Helium films adsorbed on graphite

1. use exfoliated graphite (Grafoil) to get surface areas of  $20\text{m}^2/\text{gm}$
2. homogeneous substrate ; atomically flat crystallites, typical size  $100\text{ \AA}$
3. adsorbed helium films are atomically layered
4.  $^3\text{He}$  films can be cooled as low as  $100\mu\text{K}$



helium - graphite potential



layering in helium films

Clements, Epstein, Krotscheck  
and Saarela Phys. Rev B 48, 7450  
(1993)

## Layered helium films

We consider two regimes of total coverage (= number of atoms  $\text{\AA}^{-2}$ )

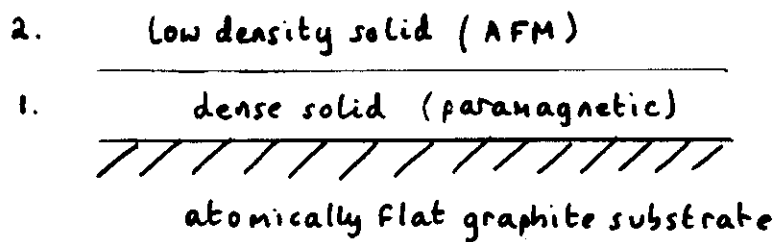
1. First layer is a dense solid ( $0.11 \text{\AA}^{-2}$ ).

**paramagnetic.**

(Can be replaced by  $^4\text{He}$ ).

Second layer forms a low density solid ( $0.064 - 0.07 \text{\AA}^{-2}$ ).

**antiferromagnetic** exchange.

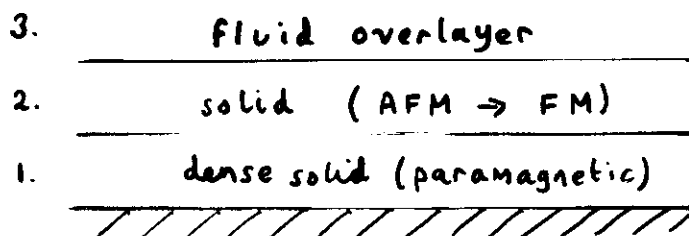


2. At higher coverages a third layer forms which is fluid.

Exchange in second layer solid evolves from

**antiferromagnetic to ferromagnetic.**

As total coverage is increased second layer is compressed slightly.



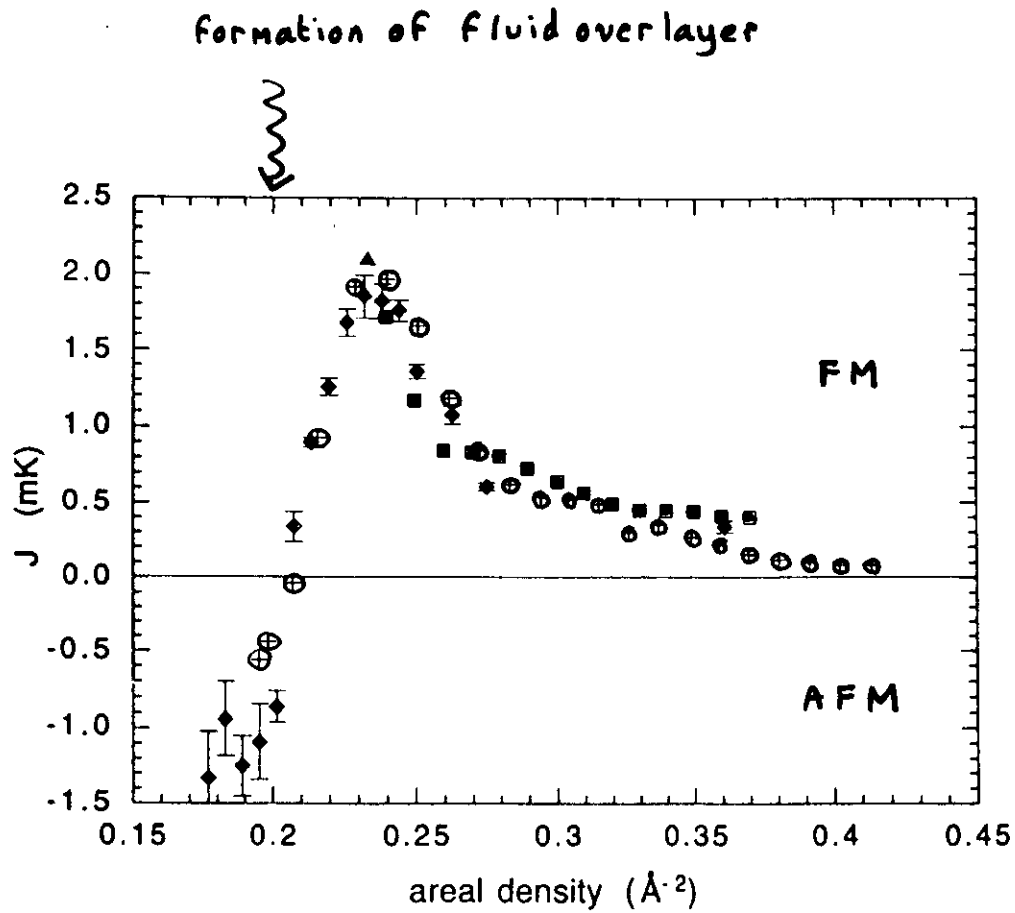
## Model two dimensional magnetic system

one solid monolayer is "magnetically active" so ideal 2D system (no "interplanar interactions")

isotropic interaction (no crystal anisotropy, exchange Hamiltonian is isotropic). Only source of anisotropy is dipolar interaction  $\sim \mu\text{K}$ .

triangular lattice (only example?)

# Magnetization of $^3\text{He}$ films; the ferromagnetic anomaly



*Composite of exchange constants: Grenoble (1994), London (1991), AT&T (1990)*

*see review by Godfrin & Rapp: Advances in Physics, 44, 113 (1995)*

## The Heisenberg magnet on a triangular lattice

Magnetic susceptibility (to leading order)

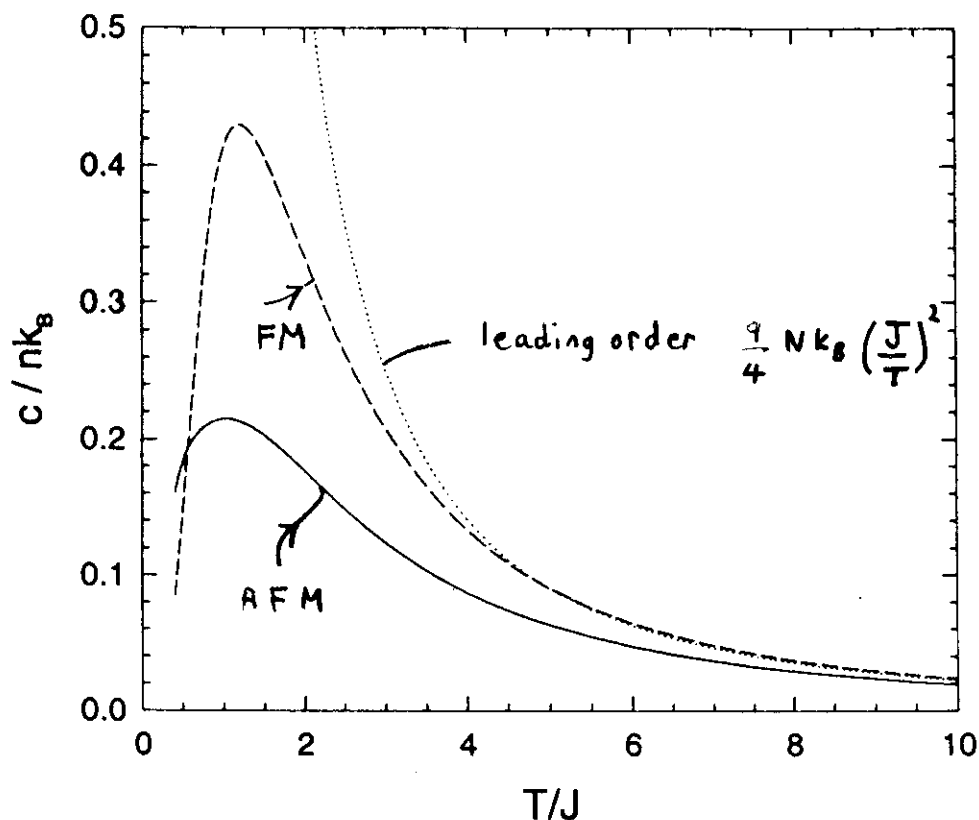
$$\chi = C/(T - \Theta) \text{ where } \Theta = +3J$$

Heat capacity (to leading order)

$$C = \frac{9}{4} N k_B \left( \frac{J}{T} \right)^2$$

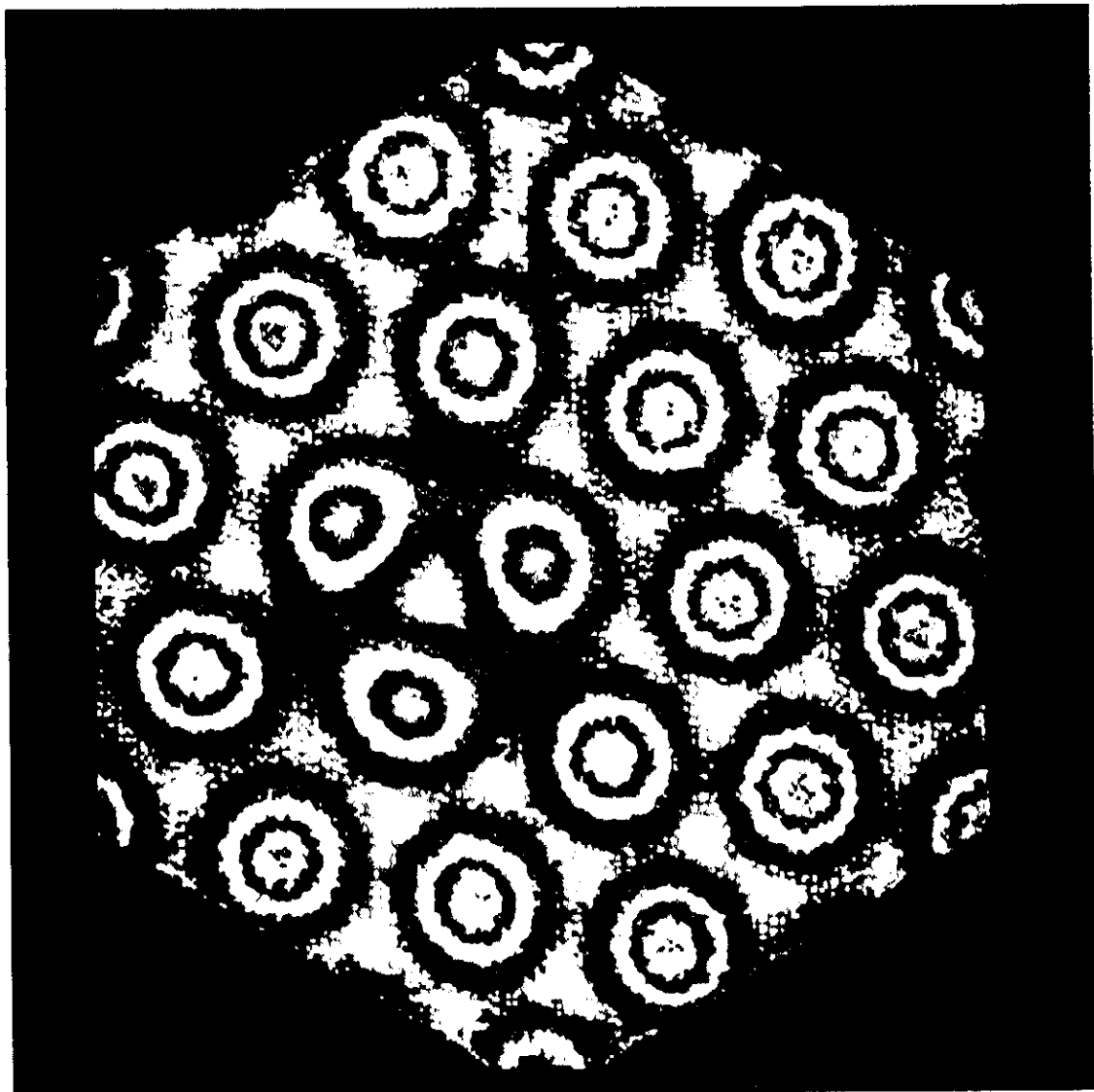
Heat capacity same for AFM or FM.

High temperature series expansions (13 terms) extended by the method of Padé approximants [N.Elstner, R.R.P Singh and A.P Young. Phys.Rev.Lett. (1993)]



⇒ ∴ Heat capacity can be used to discriminate between AFM and FM behaviour.

simulation of cyclic 3 spin exchange in 2D  $^3\text{He}$



B. Bernu & D. Ceperley  
National Center for Supercomputing  
Applications (USA) and University  
of Paris

[Roger, Hetherington, Delrieu (84); Roger (90); Ceperley and Jacucci (87); Bernu, Ceperley, Lhuillier (92)]

Competition between cyclic exchanges of odd and even numbers of particles

$$\mathcal{H} = - \sum_n (-1)^n J_n P_n \quad (\text{Thouless 1965})$$

To leading order; for 2D triangular lattice

$$\chi(T) = C/(T - \theta) \cdot \theta = 3J_\chi; \quad J_\chi = - \left( \underline{J_2 - 2J_3} + 3J_4 - 5J_5 + \frac{5}{8}J_6 \right)$$

$$\begin{array}{c} \uparrow \\ \text{measure} \\ \downarrow \\ \underline{c(T) = \frac{9}{4} N k_B \left( \frac{J_c}{T} \right)^2} \end{array}$$

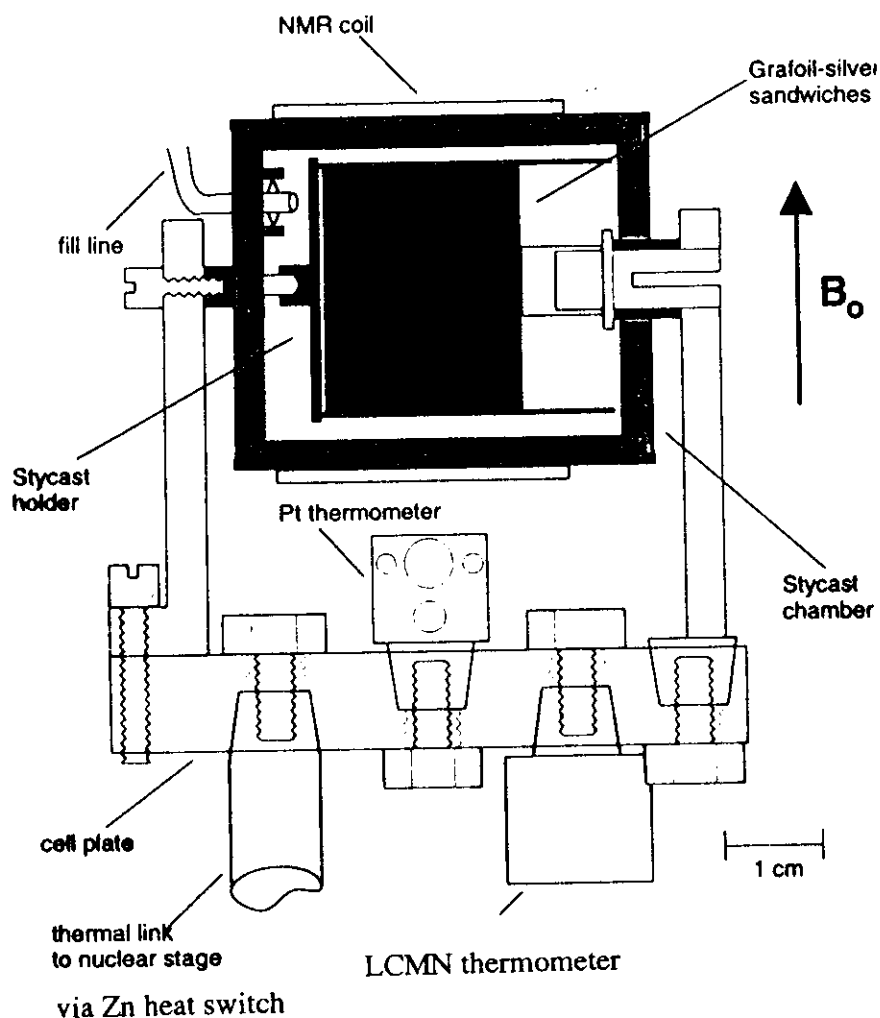
$$\begin{aligned} J_c^2 = & (\underline{J_2 - 2J_3} + \frac{5}{2}J_4 - \frac{7}{2}J_5 + \frac{1}{4}J_6)^2 + 2(J_4 - 2J_5 + \frac{1}{16}J_6)^2 \\ & + \frac{23}{8}J_5^2 - J_5J_6 + \frac{359}{384}J_6^2 \end{aligned}$$

note that if only two and three spin exchange  $J_c = J_\chi$

if  $J_2 - 2J_3 < 0$  then  $\theta > 0$ ; system is FM

but it can be driven AFM by four spin exchange

## *Sample chamber for combined NMR and heat capacity measurements*



***Grafoil sheets bonded to silver foils by Grenoble technique***

*surface area =  $182 \text{ m}^2$*

*$\dot{Q} \sim 100 \text{ pW}$*

***Continuous wave NMR at 922kHz***

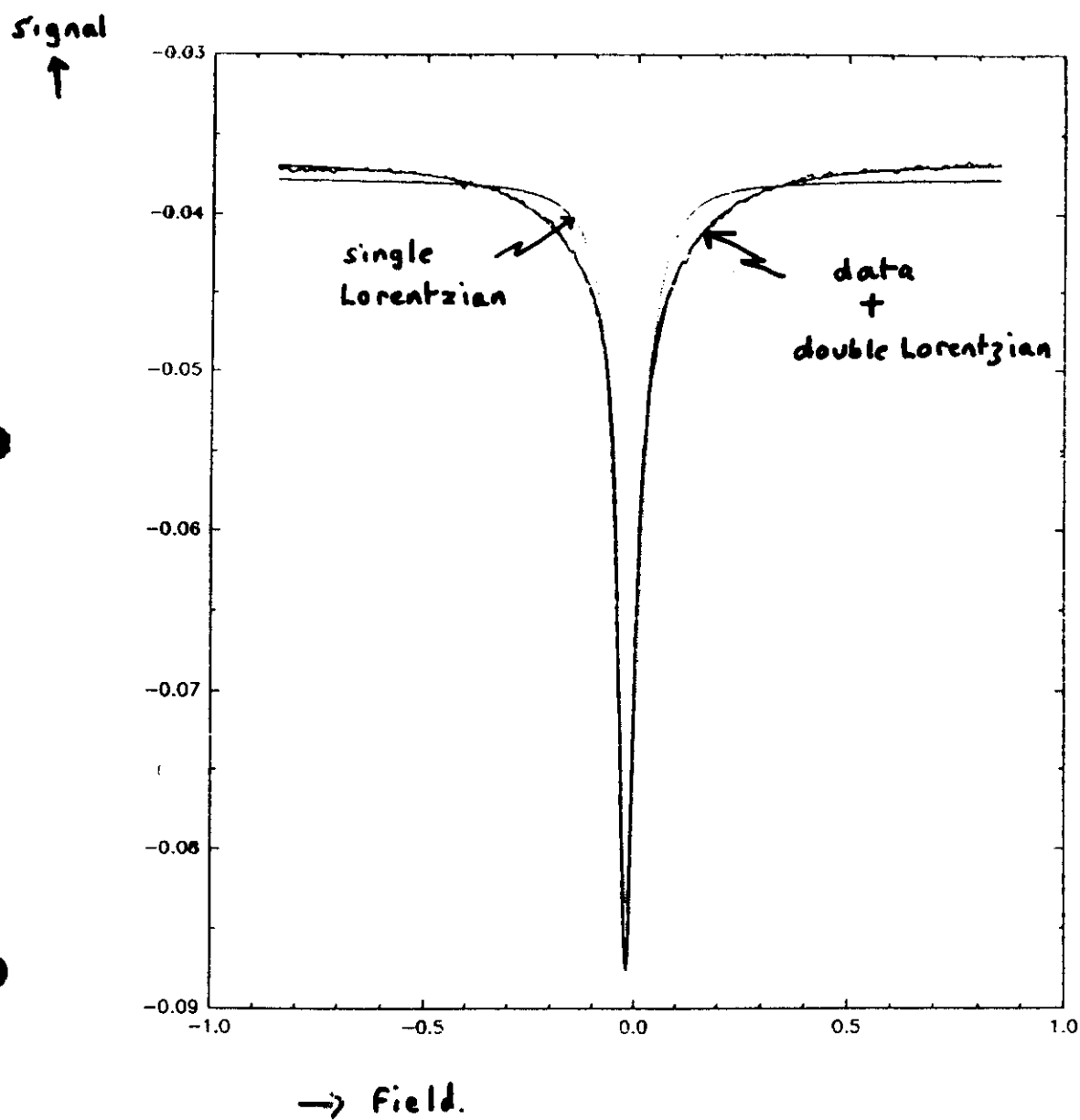
***Thermometry; LCMN (28mg) susceptibility  
(fabricated according to Greywall and Busch recipe)  
calibrated by Pt NMR and  $^3\text{He}$  melting curve.***

***Short time constant (equilibrium time < 1 minute)***

***small addendum ( <  $100 \text{ } \mu\text{J/K}$  )***

SIGNAL AFTER SOLIDIFICATION OF  
SECOND LAYER

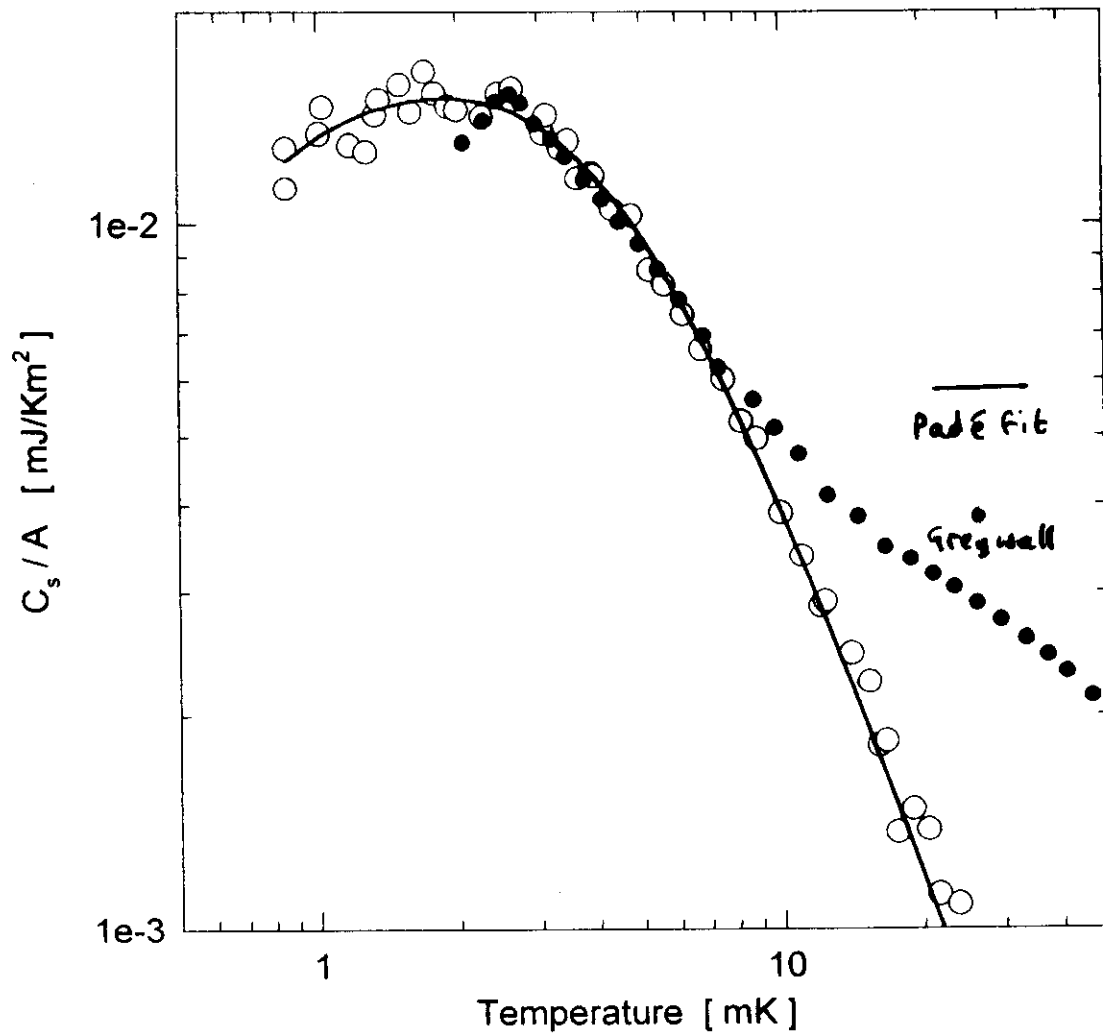
12.

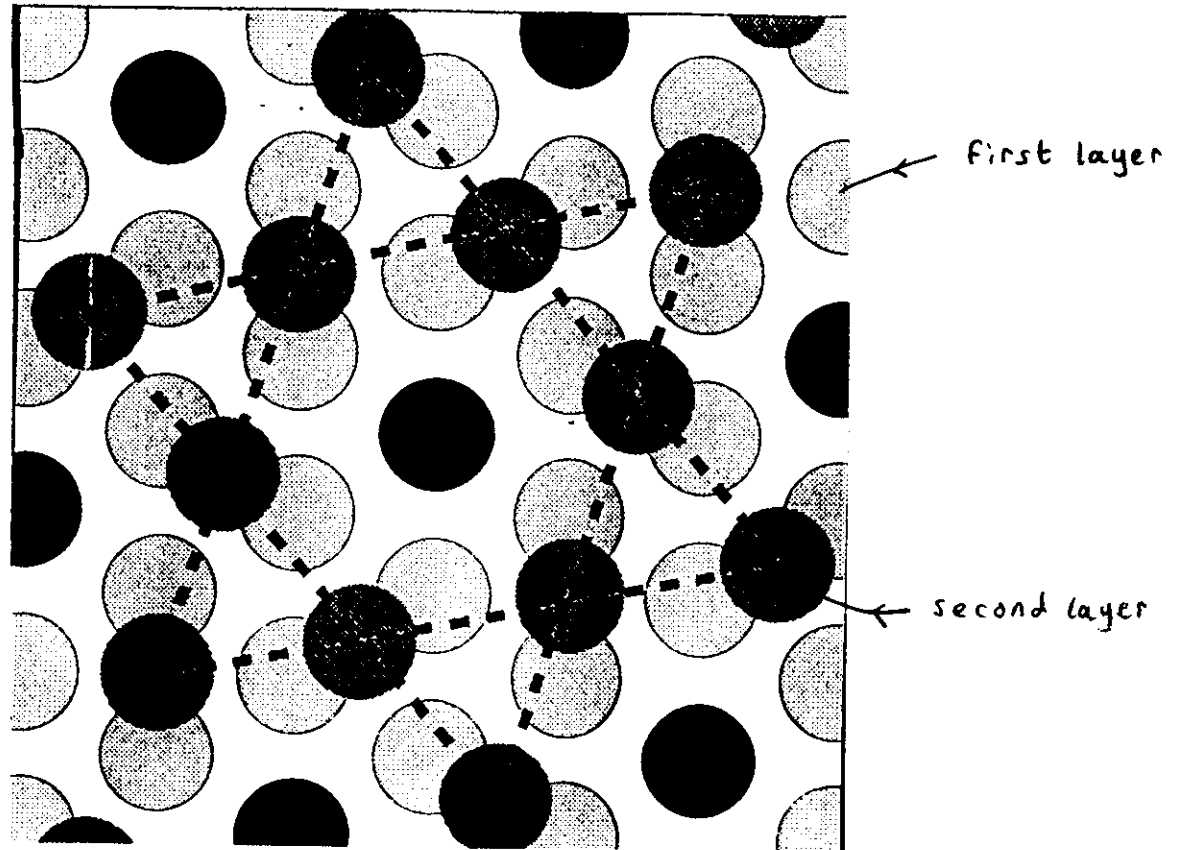


⇒ First paramagnetic layer is "inert"

ANTIFERROMAGNETIC SOLID ( $\rho = 0.178 \text{ \AA}^{-3}$ )

### Solid spins contribution per unit area





- *Triangular lattice*

- *Commensurate with first layer*

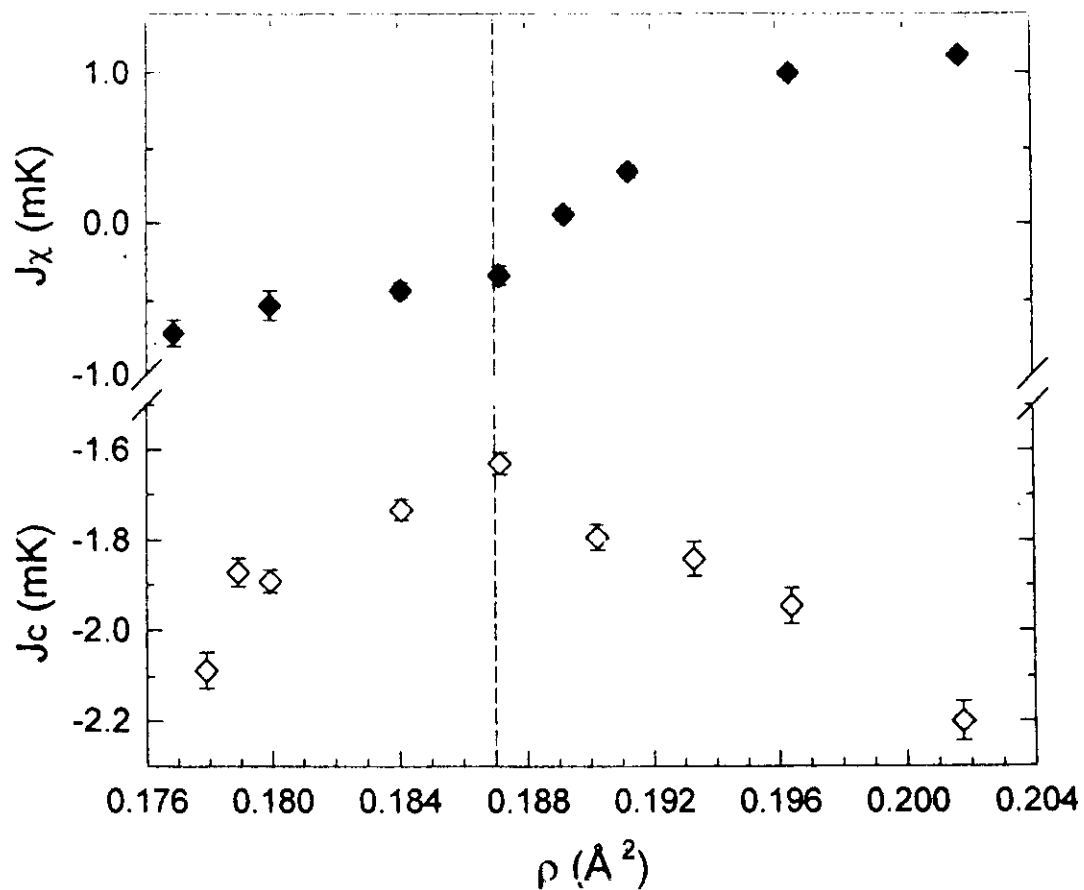
- $\rho_2/\rho_1 = 4/7$

*This proposal is supported by pre-plating experiments, (Siqueira, Lusher, Cowan Saunders).*

*In these the graphite is plated by two layers of HD, This has a density of order 20% smaller than the first  $^3\text{He}$  layer in pure films.*

*Result; shift in density at which  $^3\text{He}$  solidifies.*

## Evolution of exchange from AFM to FM



## Evidence for Multiple Spin Exchange

Different exchange constants from magnetization and heat capacity

$$J_\chi = \theta/3 \quad (\theta = \text{Curie-Weiss constant})$$

$J_c$  from fits to heat capacity

**Balance of cyclic exchange processes strongly influenced by formation of a fluid overlayer**

**$\Rightarrow$  tunable frustration**

# Understanding AFM $\rightarrow$ FM crossover

## Multiple spin exchange model ; Roger (1990)

effective exchange constant

$$J_{\chi} = \theta/3 = -(J_2 - 2J_3 + 3J_4 - 5J_5 + 5J_6/8)$$

$J' = J_2 - 2J_3 < 0$  expected from dominance of 3 spin exchange on triangular lattice

Crude model;

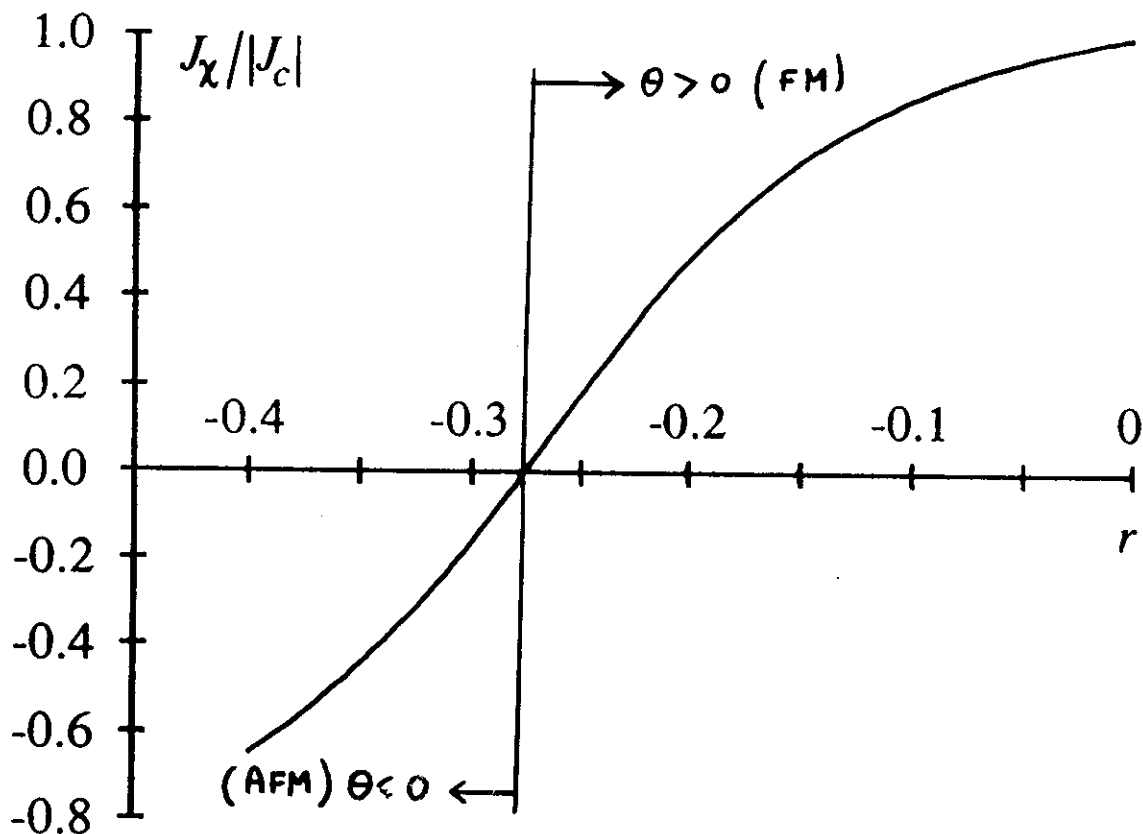
Write  $J_4 = J_6 = rJ'$  ( $r < 0$ ) with  $J_5 = 0$

$r$  is the "frustration parameter"

If  $|r|$  is big enough effective exchange constant may be driven AFM

$$J_{\chi} = -J' (1 + 3.635 r)$$

when  $r = 0$   $J_{\chi} = J_c$

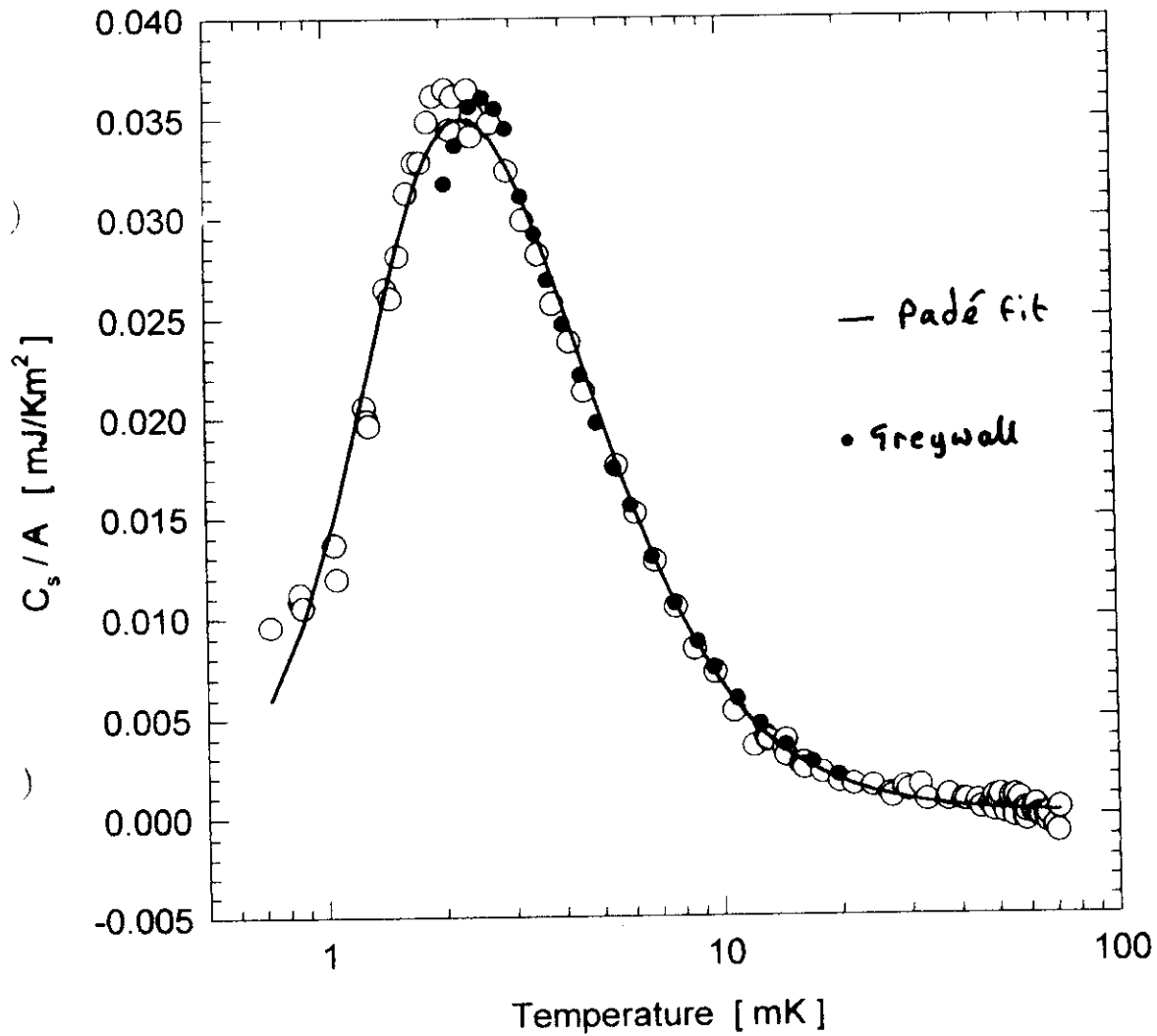


AT 'FERROMAGNETIC ANOMALY'

$$\rho = 0.24 \text{ } \text{\AA}^{-3}$$

18.

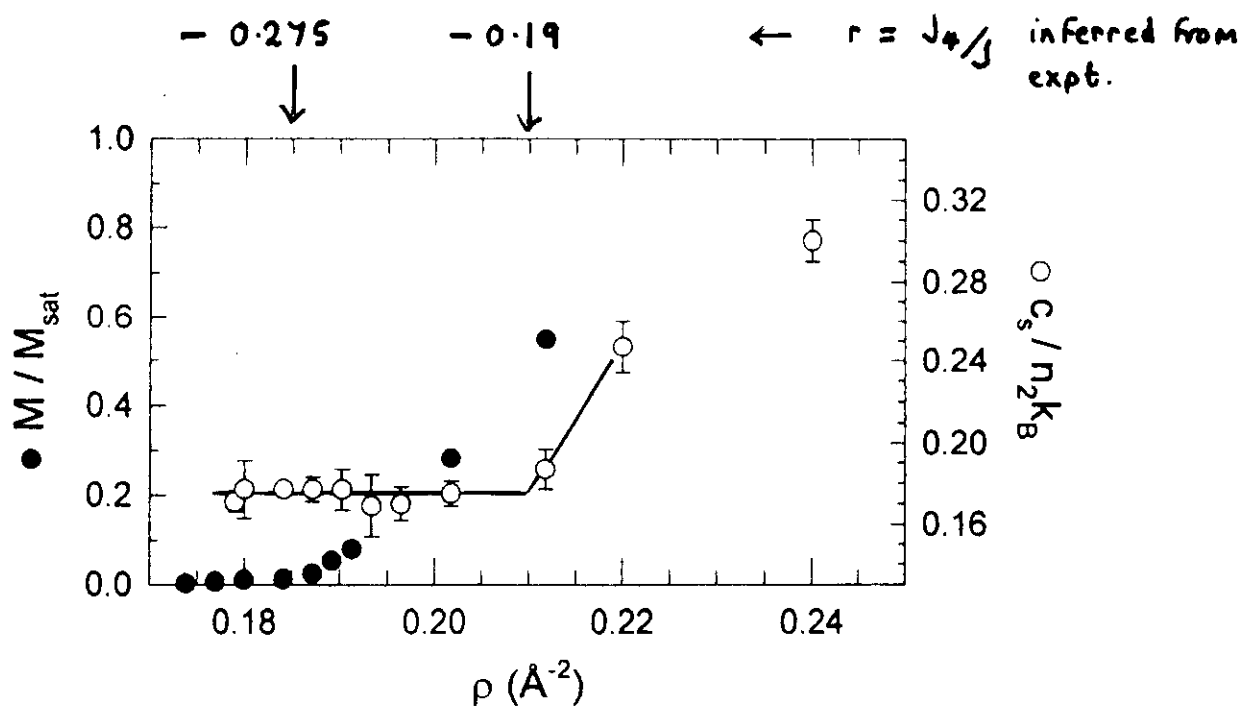
# Solid spins contribution per unit area



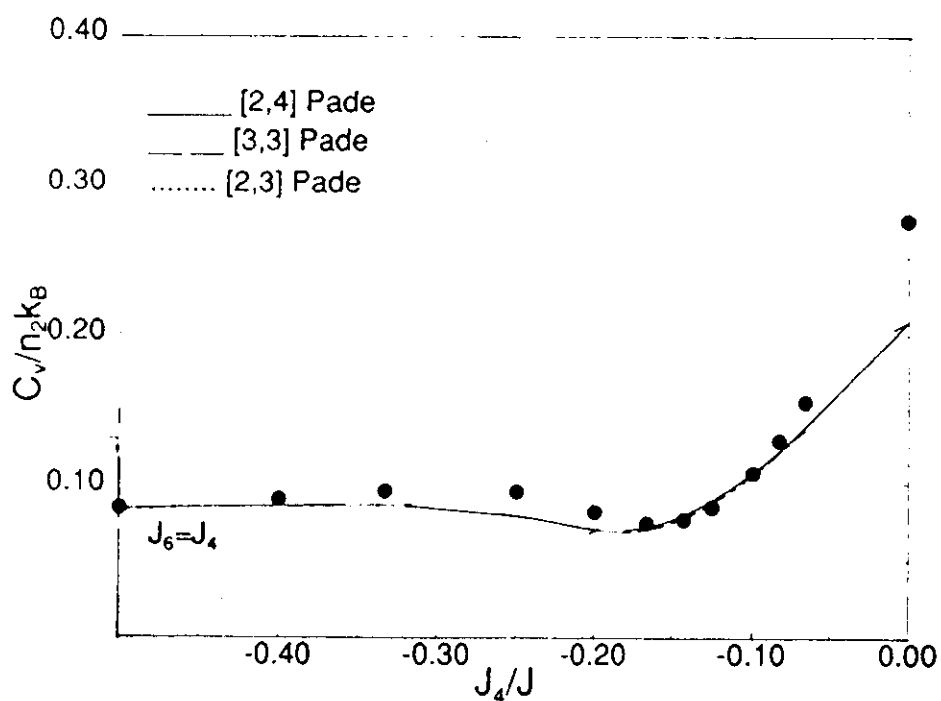
$$T_c \approx T_x \sim 2 \text{ mK}$$

## Evidence for "exotic" ground states (induced by multiple spin exchange)

(i) Experimental magnetization and heat capacity isotherms

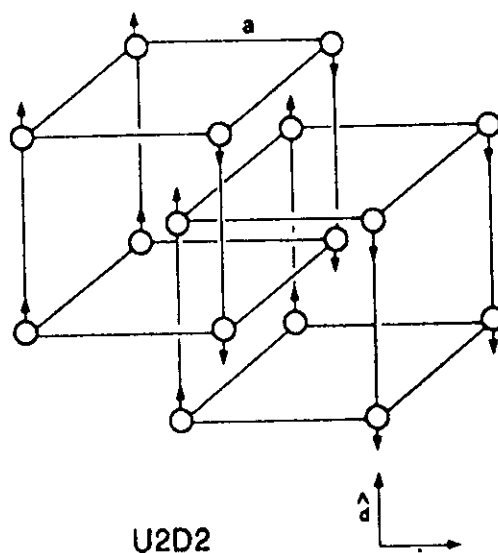


(ii) Theoretical heat capacity as a function of frustration parameter (HTSE and exact diagonalisation of  $16 \times 16$  spin cluster, Roger)

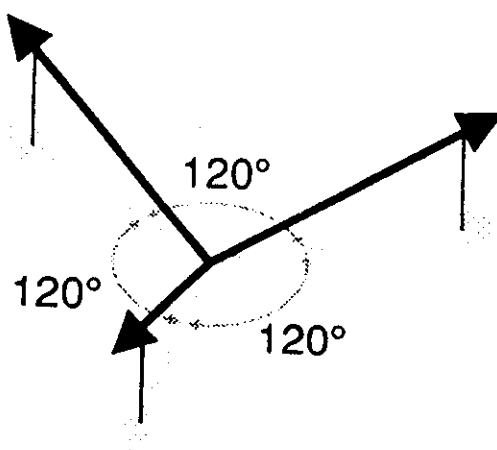


## Some ideas about ground states

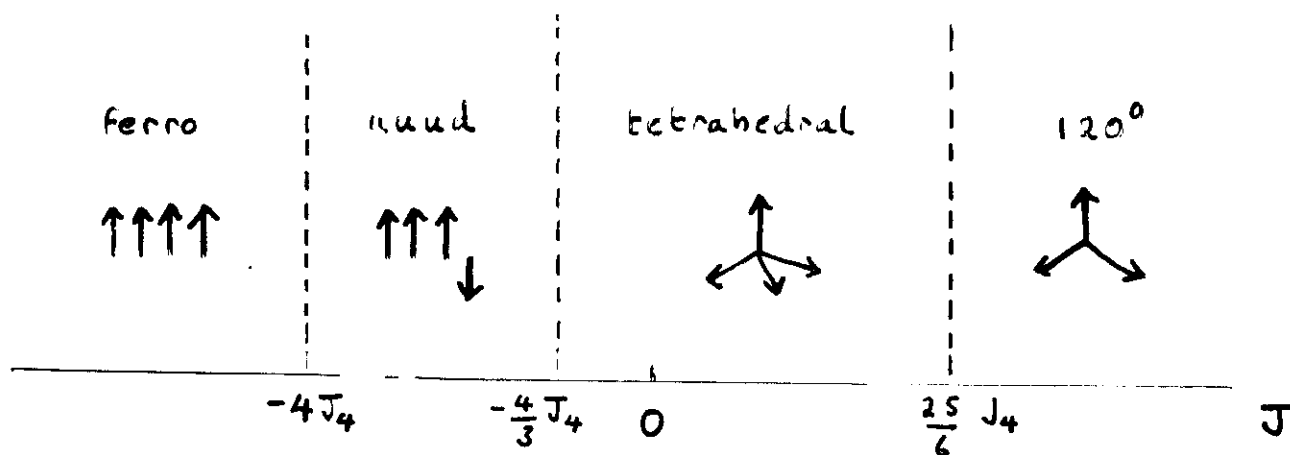
Unusual spin ordering in bcc solid  $^3\text{He}$  (u2d2) due to MSE



We proposed canted AFM in 2D



Recent calculation (K.Kubo) for classical spins in MSE model  
(3 and 4 sub-lattice equilibrium structures)

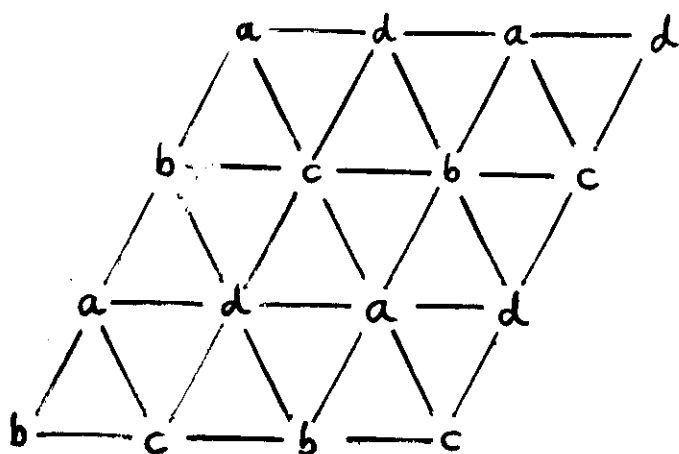


### Some consequences

1.  $T = 0$  order is tuned by the frustration
2. A finite temperature phase transition is possible for two of these states.

$120^\circ$  state; topological phase transition

tetrahedral state;



4 sublattices

order parameter  $S_1 \cdot (S_2 \times S_3)$

# Low frequency NMR using DC SQUIDS

## System parameters;

1.7 m<sup>2</sup> Grafoil

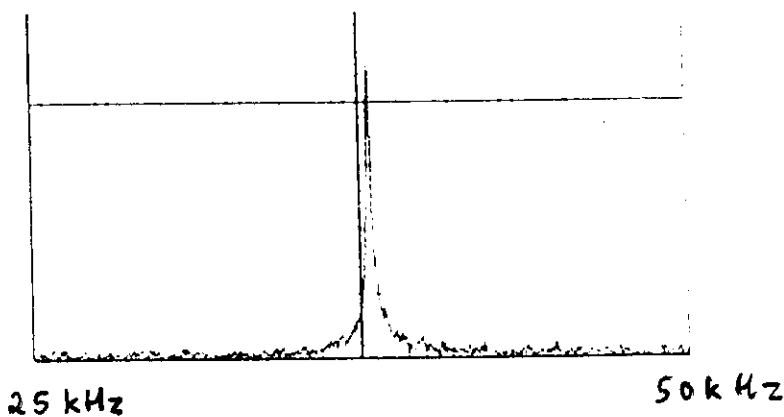
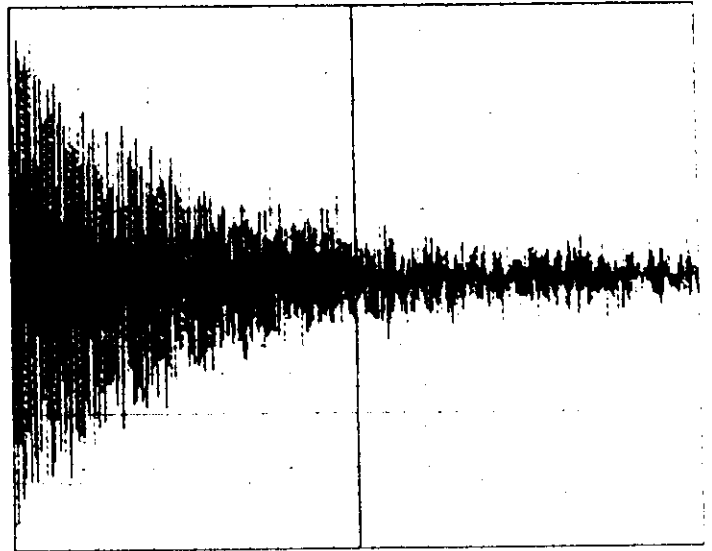
10<sup>18</sup> spins

T=1.5K (so signal of order 10<sup>6</sup> smaller than saturation magnetization)

applied field 12 gauss (  $\nu_0 = 38\text{kHz}$  )

signal/noise  $\sim 0.3$  in a single shot

*Free induction decay*



**objective:** NMR in zero field. Spins resonate in local dipolar field, providing signature of ordered state.

### 1. Quantum antiferromagnetism

*Second layer provides model  $S=1/2$  system on a triangular lattice*

*Heat capacity well described by HTSE for HAFT (first example)*

*No phase transition: no anomalous  $c(T)$*

*Measure effective exchange constants from both heat capacity and magnetization to obtain quantitative measure of frustrated multiple spin exchange*

### 2. Frustrated exchange

*Fluid overlayer shifts delicate balance between different exchange processes, so we can tune frustration*

*We can begin to account for different coverage dependences of heat capacity and magnetization, within MSE model*

*At FM anomaly, system is essentially Heisenberg. We now have consistency with magnetization data*

*Evidence for new ground states at intermediate coverages*

*AFM  $\rightarrow$  canted AFM  $\rightarrow ? \rightarrow$  FM*

### 3. Future

*Require more theory for ground state and finite  $T$  properties within MSE*

*Further work to establish ground state order in AFM phases*

*Topological phase transition?*

## Nuclear magnetism of two dimensional solid $^3\text{He}$

Marcio Siqueira, Jan Nyéki\*, Brian Cowan and John Saunders†

Department of Physics, Royal Holloway University of London, Egham, TW20 0EX, UK

The properties of two dimensional frustrated magnets have been studied in an investigation of the nuclear magnetism of two dimensional solid  $^3\text{He}$ . The results of recent heat capacity and NMR measurements on  $^3\text{He}$  films adsorbed on graphite are reported. The coverage dependence reveals both antiferromagnetic and ferromagnetic regimes and their description in terms of Heisenberg series expansions is discussed. There is clear evidence of frustration by multiple spin exchange, with no magnetic phase transition. 2D  $^3\text{He}$  currently provides the best model system for the study of  $S=1/2$  quantum antiferromagnetism on a triangular lattice. There is evidence that the frustration can be tuned, and hence the ground state order.

### 1. Introduction

Two dimensional magnetic systems with Heisenberg spin exchange can only exhibit long range magnetic order (LRMO) of the Néel type, corresponding to broken continuous symmetry, at  $T=0$ . Considerable theoretical attention has been devoted to the problem of the ground state of quantum antiferromagnets. While it is believed that the spin  $1/2$  antiferromagnet on a square lattice exhibits conventional LRMO, albeit with staggered magnetization significantly reduced by quantum fluctuations from the classical value, the ground state of the  $S=1/2$  Heisenberg antiferromagnet on a triangular lattice (HAFT) is more controversial. The particular importance of this lattice is that it offers the simplest example of geometrical frustration; on the elementary triangle it is impossible to arrange all three spins so that they are mutually antiparallel. Another example is the *kagomé* lattice, consisting of corner sharing triangles, in which the geometrical frustration is most extreme. Geometrical frustration is also possible in certain 3D lattices [1].

The possibility exists that this frustration will give rise to unconventional ground states such as the quantum spin liquid. However it seems that the weight of theoretical evidence points to the existence of LRMO on the triangular lattice [2]. For classical spins the ground state is a three sublattice non-collinear spin structure in which the angle between nearest neighbour spins is  $120^\circ$  thereby releasing the frustration. For  $S=1/2$  quantum fluctuations suppress the local moment, but again there is

theoretical controversy over the degree.

Another source of frustration in these systems arises from an increase in the complexity of the spin exchange. This has been explored for  $S=1/2$  on a square lattice by adding next nearest neighbour and third nearest neighbour coupling or cyclic four spin exchange. This generates a rich phase diagram with regions of collinear, canted and dimerized order [3].

The challenge for experimentalists is to identify physical systems to test these ideas. As far as the triangular lattice is concerned there is a real lack of suitable quasi-two-dimensional materials with isotropic spin exchange. The first system to be proposed was  $\text{NaTiO}_2$  [4], which has  $S=1/2$ . Since then the search has continued, with new candidate materials [5] but so far none with  $S=1/2$ .

In this paper we discuss experiments which show that atomic layers of  $^3\text{He}$  adsorbed on graphite provide a model system for studying the  $S=1/2$  HAFT. This physical system is genuinely two dimensional. The only source of anisotropy is the dipolar interaction which is weak. As well as the geometrical frustration associated with the triangular lattice, we demonstrate that cyclic exchange processes are important. This provides a further source of frustration, which is tunable by varying the coverage of the helium film. This of great interest since, as we have seen, the frustration may be expected to affect strongly the ground state order. A further flexibility is offered by the possibility of pre-plating the graphite surface with a discrete number of monolayers of another gas, to alter the binding potential. In general this is expected to influence the exchange rates.

† corresponding author: j.saunders@rhmc.ac.uk

\*permanent address: Institute of Experimental Physics, Slovak Academy of Sciences, Kosice.

## 2. Exchange in adsorbed helium films

In quantum solids the large atomic zero point motion leads to the interchange of atoms between sites. The rate is much smaller than the Debye frequency so the picture of a spatially ordered solid is preserved. The short range repulsive potential between atoms, which can be pictured as hard spheres, results in a larger exchange rate for the cyclic permutation of three particles than for the simple interchange of two particles, simply because the atomic wavefunctions are less "squeezed" during exchange. (This "squeezing", sometimes referred to as steric hindrance, costs zero point energy). Higher order cyclic exchange processes are also important. Since  $^3\text{He}$  has nuclear spin  $1/2$ , these processes lead to an effective nuclear spin-spin interaction. In general, as first shown by Thouless [6], the Hamiltonian is  $H = -\sum_n (-1)^n J_n P_n$  where  $P_n$  is the cyclic permutation operator for  $n$  particles, and  $J_n$  are the exchange constants. (All  $J_n$  are positive according to this definition). For two and three particle exchange this Hamiltonian is of the Heisenberg form. Exchange of an even number of particles is antiferromagnetic, while that of an odd number is ferromagnetic, so the spin exchange is frustrated. This is the basis of the so-called multiple spin exchange (MSE) model [7]. It is important to note that typically the exchange constants are large, of order mK and at least a factor  $10^3$  greater than the nuclear exchange interactions in the most extensively studied bulk metallic systems Cu and Ag [8]. In solid  $^3\text{He}$  the wide separation of the exchange energy and the dipolar energy (of order  $\mu\text{K}$ ) make it a particularly attractive model system.

MSE models the "scrambling of atoms among lattice sites" [9]. (It has been argued that fundamentally this results from the creation of virtual vacancy-interstitial pairs [10]). Importantly the exchange constants for the various cyclic exchange processes can be calculated explicitly, by path integral Monte Carlo methods, with the helium interatomic potential as input [10, 11]. In 2D, calculations have been done taking full account of the delocalisation of the particle wave functions normal to the surface; the surface binding energy significantly influences the exchange rates [12].

Helium films grown on the surface of graphite are atomically layered [13]. In pure  $^3\text{He}$  films the first layer forms a compressed incommensurate triangular lattice with very weak exchange. The heat capacity measurements of Greywall [14] first showed that at low densities the second layer forms a Fermi fluid; as the density is increased a coexistence region is entered, the layer completely solidifying at a density of  $0.064\text{\AA}^{-2}$ . It is believed that this solid forms a triangular lattice commensurate with the first layer. A structure has been

proposed (Fig. 3) in which the ratio of the densities of the first and second layers is  $\rho_2/\rho_1 = 4/7$ , consistent with the measurements [15].

Partly to test this hypothesis experiments were performed on graphite preplated by a bilayer of HD [16], thereby reducing the density of the underlayer by 20%. NMR and heat capacity measurements find that the first helium layer solidifies at a coverage that is consistent with the commensurate solid hypothesis. Heat capacity melting peaks of this solid have recently been observed [17] (with a bilayer of hydrogen preplating). Commensuration effects therefore seem to be important in stabilising low density 2D solids in these films, and this has received support from Monte Carlo calculations [18].

In pure  $^3\text{He}$  films the exchange rate between the first and second layer is negligible, being comparable to or smaller than the dipolar interaction. This is clear from the observed lineshape which is very well described by the sum of two Lorentzians; fast exchange would give rise to a single Lorentzian. This places an upper bound on the interlayer exchange rate of order 10kHz. However since the ratio of the magnetizations of the two layers is temperature dependent the linewidth of both components is also temperature dependent (note that these components cannot simply be identified with the first and second layer).

A second piece of evidence in support of the passive role of the paramagnetic first layer in exchange in the film is that when it is replaced by a monolayer of  $^4\text{He}$  the measured exchange constants agree well with results on pure  $^3\text{He}$  films [19]. Note that the pre-plating relies on the preferential adsorption of  $^4\text{He}$  at the graphite surface, due to its lower zero point energy.

At higher coverages promotion to a fluid overlayer occurs (at a density of the second layer of around  $0.07\text{\AA}^{-2}$ ). Below this coverage we are dealing with a single magnetically active monolayer and thus need only consider intralayer exchange. Preplating the graphite with an HD bilayer allows a wider range of densities of this 2D solid monolayer to be accessed, as well as eliminating the background magnetization of a first paramagnetic layer, as with  $^4\text{He}$  preplating. Thus the second layer of  $^3\text{He}$  films on bare graphite, the first layer on graphite plated with a monolayer of  $^4\text{He}$  or a bilayer of hydrogen, are related systems with a single "magnetically active" solid layer. In pure  $^3\text{He}$  films following promotion the second layer continues to be compressed, while on the HD pre-plated substrate there is evidence that the solid layer is de-compressed once a fluid overlayer forms.

In this paper we will show that the presence of the

fluid overlayer shifts the balance of different exchange processes. This could arise from its influence on the steric hindrance of intralayer exchange (acting as a "blanket" over the exchanging second layer atoms), or by the introduction of a new exchange pathway, indirect interlayer exchange of the RKKY type mediated by the fluid overlayer [13]. In the present work we are unable to distinguish these two possibilities. Variations in either interlayer or intralayer exchange can be regarded as providing equivalent means of continuously tuning the frustrated spin exchange.

### 3. Frustrated spin exchange

The seminal paper of Roger [20] emphasises the importance of MSE in 2D solid  $^3\text{He}$ . Measurements of both the heat capacity and magnetization are important to determine the degree of frustration, since different combinations of the exchange constants  $J_n$  enter into these quantities; the high temperature behaviour can be characterised by two effective exchange constants  $J_X$  and  $J_C$ . To leading order the magnetic susceptibility is given by  $\chi = C/(T - \theta)$ , where  $\theta = 3J_X$ , while the heat capacity is  $c = (9/4)Nk_B(J_C^2/T^2)$ .

For a Heisenberg magnet with nearest neighbour exchange constant  $J$ , then simply  $J_X = J_C = J$ . It is apparent that a measurement of  $\theta$  determines the sign of  $J$ , and therefore distinguishes between AFM and FM exchange. However the character of the exchange can also be determined from the full temperature dependence of the heat capacity measured to  $T \sim J$  [21]. Recently high temperature series expansions (HTSE) to order 13 or 14 in  $J/T$  and extended by the method of Padé approximants, have been derived for a triangular lattice [22] (Fig. 1). These show a heat capacity maximum associated with short range order at  $T \sim J$ , the height of which differs by a factor of about two depending on the sign of  $J$ . For the AFM, the heat capacity per spin at the maximum is  $0.21k_B$ . It is of interest to note that the heat capacity converges more slowly toward the asymptotic  $1/T^2$  behaviour in the AFM case.

In the case of MSE, if only two and three spin exchange are taken into account then the system is equivalent to Heisenberg nearest neighbour with effective exchange constant  $J' = J_2 - 2J_3$ , and  $J_C = J_X = -J'$ . However, while in the 2D films studied so far  $J'$  appears to be negative under all conditions showing that three spin exchange dominates pair-wise exchange, as might be expected on a triangular lattice, higher order cyclic exchanges can drive the system antiferromagnetic. The experimental signature of the importance of such processes is differing values of  $J_C$

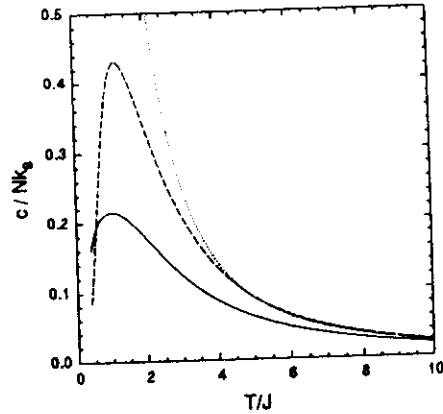


Fig. 1 Theoretical heat capacity for Heisenberg nearest neighbour exchange on a triangular lattice, ref. [22]. AFM (solid line), FM (dashed line). Dotted line shows leading order  $1/T^2$  behaviour.

and  $J_X$ , which depend on different combinations of the  $J_n$  [20]. Thus  $J_X = -(J_2 - 2J_3 + 3J_4 - 5J_5 + 5J_6/8)$ , while

$$J_C^2 = \left(J_2 - 2J_3 + \frac{5}{2}J_4 - \frac{7}{2}J_5 + \frac{1}{4}J_6\right)^2 + 2\left(J_4 - 2J_5 + \frac{1}{16}J_6\right)^2 + \frac{23}{8}J_5^2 - J_5J_6 + \frac{359}{384}J_6^2$$

For the present discussion we adopt Roger's simplified model [20] in which it is assumed that  $J_4 = J_6$  and five spin exchange is neglected. There is then a single frustration parameter  $r$ , defined by  $J_4 = rJ'$  (note that  $r < 0$ ) and a measurement of  $J_C$  and  $J_X$  can determine both  $r$  and  $J'$ .

In the following we present results for heat capacity and magnetization, from which we have been able to infer both  $J_C$  and  $J_X$ , and hence arrive at a direct measure of the frustration. We argue that there is persuasive experimental evidence that the above MSE model accounts for the essential physics of this system.

### 4. Experimental details

Our experimental set-up allows heat capacity and NMR measurements to be performed on the same cell, for the first time for 2D  $^3\text{He}$ . The substrate consists of a stack of 0.15mm thick Grafoil sheets, baked at  $1100^\circ\text{C}$  in vacuum and then diffusion bonded to silver foils of thickness 0.025mm at  $650^\circ\text{C}$  using the Grenoble technique [13]. The foils are diffusion welded to a silver post; thermal contact between this and the cell plate is made by a mechanical cone joint. The total surface area for adsorption was determined to be  $89\text{m}^2$  by the following procedure. Second layer promotion was identified both by an NMR linewidth isotherm at 10mK and a vapour pressure isotherm at 4.2K with an agreement of better than 1%; for our cell promotion corresponded to 36.2 STP cc of gas. We assume

promotion to occur at  $0.109\text{\AA}^{-2}$ , primarily to facilitate comparison with previous results [14].

Mounted on the cell plate is an LCMN thermometer constructed in a similar way to the CMN thermometer described by Greywall and Busch [23]. The lanthanum dilution was 95% and the total mass of salt  $\sim 28\text{mg}$ . This thermometer was chosen for the following characteristics: continuous readout of temperature, negligible self or sample heating, small addendum, good precision over a wide temperature range when used in a mutual inductance bridge with a rf-SQUID null detector. It was calibrated against a platinum wire NMR thermometer mounted on the cell plate and, at higher temperatures, a melting curve thermometer mounted on the nuclear refrigeration bundle. The magnetic susceptibility of the LCMN thermometer obeyed a Curie-Weiss law to  $0.5\text{mK}$ , with a Curie-Weiss constant of  $-0.5\text{mK}$ . This relatively high value presumably arises from the effects of compression of the LCMN crystals required in construction of the thermometer. Thermal connection between the cell plate and the bundle is via a zinc superconducting heat switch. Heat capacity is measured by the standard adiabatic method; magnetization measurements were made by standard field-swept continuous wave NMR methods.

## 5. Pure $^3\text{He}$ films

### 5.1 Quantum antiferromagnetism

Heat capacity isotherms establish that the second layer completely solidifies at a coverage  $0.178\text{\AA}^{-2}$ , in complete agreement with earlier results [14]. We find promotion to a third layer occurs at  $0.187\text{\AA}^{-2}$ , a little higher than the previous value. Taking the density of the compressed first solid layer to be  $0.114\text{\AA}^{-2}$ , this corresponds to a density range for the second layer solid of  $0.064$  to  $0.073\text{\AA}^{-2}$ , before the onset of layer promotion and the formation of a fluid overlayer.

The heat capacity of the second layer in this régime is shown in Fig. 2. The contribution of the first layer to the total heat capacity is negligible. The data can be extremely well described by the HTSE for Heisenberg nearest neighbour AFM on a triangular lattice [22]. The fits shown are to  $c = Nk_B \text{PA}[J/T] + \beta$ , where the first term is the Padé approximant for the AFM spins, with effective exchange constant  $J$ , and the constant term  $\beta$  is believed to arise from weak heterogeneity of the substrate [14]. The value of  $N$ , the number of AFM spins, inferred from the fit is in excellent agreement with the total number of second layer spins,  $N_2$ . This is powerful evidence that the spins are arranged on a triangular lattice. We identify the energy scale

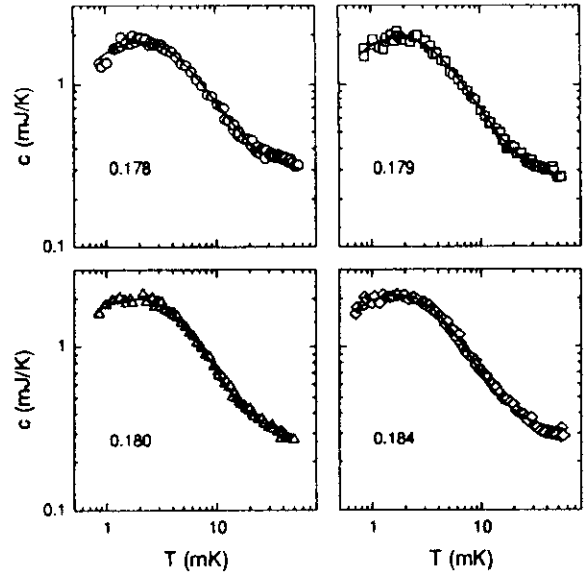


Fig. 2 Heat capacity of AFM second layer, at total coverages shown, with fits to theory for a  $S=1/2$  HAFT, see text.

characterising the temperature dependence of the heat capacity with  $J_c$ . Over this density range  $|J_c|$  decreases from  $2.1\text{mK}$  to  $1.6\text{mK}$ . These results are in marked contrast with previous work [14] in which a sharp coverage independent peak was observed at  $2.5\text{mK}$ , attributed to an unexpected finite temperature phase transition. In contrast our results are entirely consistent both in magnitude and temperature dependence with that predicted for a HAFT, the broad maximum being associated with short range magnetic order. Clearly this result motivates the calculation of HTSE within the MSE model.

If we extrapolate our data linearly to  $T=0$  we determine a residual entropy of between  $0.2k_B \ln 2$  and  $0.25k_B \ln 2$  (neglecting the contribution of  $\beta$ ), depending on coverage. This is close to the value obtained by performing the same procedure on the Padé expression for the heat capacity, and it reflects the presence of a large density of low lying states, which are a consequence of the geometrical frustration. Heat capacity measurements to significantly lower temperatures will be required to explore these. The residual entropy found here is smaller than that determined by Greywall [14] (of order  $0.5k_B \ln 2$ ). That result provoked a model [15], in which it was proposed that the commensurate triangular lattice should be thought of as a *kagomé* net, involving  $3/4$  of the spins on equivalent sites, the remaining  $1/4$  of the spins occupying a different set of equivalent sites (Fig. 3). According to this model these latter spins are free, having only weak exchange with those on the *kagomé*

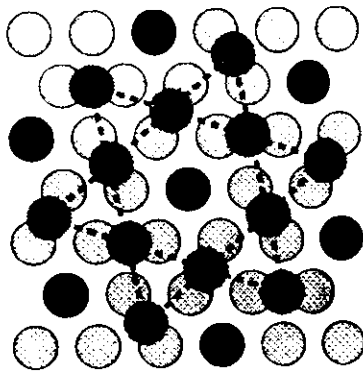


Fig. 3. Second layer triangular lattice (darker spheres) in commensuration with first layer triangular lattice (lighter spheres) as proposed by Elser [15],  $\rho_2/\rho_1 = 4/7$ . Unit cell of kagomé lattice, populated by 3/4 of second layer atoms, is also shown.

net. However the present heat capacity data are inconsistent with this model since it is known from HTSE that the heat capacity maximum for the kagomé net corresponds to  $0.19k_B$  per spin [24] and only 75% of the spins of the second layer lie on the net. Clearly the predicted heat capacity falls significantly below that observed.

In order to infer the second layer magnetization, a large Curie law contribution from the first layer must be subtracted. This we determined by performing measurements on the two layer system at coverages just before solidification of the second layer. After second layer solidification measurements are complicated by the double Lorentzian lineshape referred to earlier, the linewidth of both components increasing significantly with decreasing temperature. Fitting the data to the HTSE above 2mK, we determine an exchange constant  $J_\chi$  close to  $-0.5\text{mK}$  [25], see Fig. 5. The exchange constants are in good agreement with those obtained earlier with a  $^4\text{He}$  preplated substrate [19], where no magnetic background subtraction is necessary. They are significantly smaller, by a factor close to three, than early values reported by the Grenoble group [26]; more recent data from Grenoble which agree well with our results are discussed elsewhere in these proceedings [27]. The magnetization data also indicate that all second layer spins participate in the exchange and are inconsistent with the presence of 25% free spins in this layer, as discussed in more detail elsewhere [25].

The fact that  $J_\chi$  is much smaller than  $J_c$  is direct evidence of the importance of frustrated spin exchange. According to the simplified model discussed earlier the ratio  $J_\chi/J_c$  determines  $r$  to be close to  $-0.3$ . Although both effective exchange constants decrease with increasing coverage, the frustration (and hence the balance of exchange processes) appears to be only

weakly coverage dependent. This is reminiscent of bulk solid  $^3\text{He}$ , where the various cyclic exchange constants appear to have a very similar strong dependence on lattice parameter [28]. We find that in 2D however, this dependence is considerably weaker, perhaps supporting the view that the creation of virtual vacancies is the process at the heart of MSE.

These measurements show that the second layer of helium forms a triangular lattice, stabilised by commensuration effects: a model quantum antiferromagnet. Exchange is driven antiferromagnetic by fourth and higher order cyclic spin exchange. Commensuration appears not to have a significant effect on the exchange, and as one moves away from exact commensuration any lattice distortion does not seem to have a detectable influence on the thermodynamic properties.

## 5.2 Tuning the frustration

### (i) The ferromagnetic anomaly

Perhaps the most extraordinary property of these  $^3\text{He}$  films is that the exchange can be driven from AFM to FM, simply by increasing the coverage. It was first demonstrated by Godfrin and co-workers [29], that as the coverage is increased to form a third (fluid) overlayer the second layer magnetization develops a FM tendency. There is a maximum in the FM exchange constant near  $0.24\text{\AA}^{-2}$ , referred to as the "ferromagnetic anomaly". Measurements of the magnetization are well described by HTSE for a Heisenberg FM [31], and behaviour at  $T < J$  is understood in terms of two dimensional FM spin waves [30, 31, 32]. We now have a model 2D ferromagnet.

A puzzling feature of previous heat capacity data at the anomaly [14] was that they were *not* well described by the Heisenberg nearest neighbour Hamiltonian. By contrast the present results are *extremely well* described by FM HTSE. The total heat capacity is fit by  $c = Nk_B P_A[J/T] + \gamma T + \beta$ , where the additional term linear in  $T$  arises from the Fermi fluid overlayer. In Fig. 4 we show the second layer spin heat capacity and the associated fit. The fit extends down to  $T/J \sim 0.5$  and gives a value of  $J_c = 1.9\text{mK}$ , close to the value of  $J_\chi \approx 2\text{mK}$  [13] obtained from magnetization measurements. The fitted number of second layer spins corresponds to  $0.075\text{\AA}^{-2}$ , in agreement with previous measurements of the second layer density from magnetization studies [19]. More details can be found elsewhere in these proceedings [33]. The similarity of  $J_c$  and  $J_\chi$  shows that at the anomaly frustration effects are weak, with  $-0.1 < r < 0$ . The inferred number of FM spins indicates that all the second layer spins

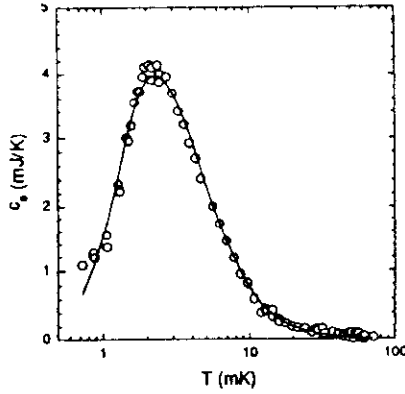


Fig. 4. Spin heat capacity at the ferromagnetic anomaly,  $0.24\text{\AA}^{-2}$ , with fit to Padé approximant to FM HTSE. No evidence of a finite  $T$  phase transition. All the second layer spins participate in the FM exchange. Effective exchange constant is  $1.9\text{mK}$ .

participate in FM exchange. Moreover there is no indication of a sharp peak indicative of a phase transition, as reported previously [14] and unexpected in a pure Heisenberg 2D FM. A number of serious inconsistencies between previous heat capacity and magnetization measurements are thereby resolved. Extrapolating the spin heat capacity at the lowest temperatures linearly to  $T = 0$  and integrating we find an entropy per spin of  $1.05k_B \ln 2$ , close to the value expected. There is no “residual entropy” as found in the AFM regime.

(ii) *Transition from anti- to ferro- magnetic exchange*

We now ask: what is the physical mechanism behind the crossover from AFM to FM behaviour? We find clear evidence for the influence of the fluid layer on the balance of exchange processes.

Measuring the heat capacity and magnetization we are able to locate a distinct break in the coverage dependence of both  $J_x$  and  $J_c$  at precisely the coverage corresponding to promotion to a fluid overlayer (Fig.5). Shortly after promotion the magnetization data indicates FM exchange. What is at first sight remarkable is the appearance of both AFM and FM tendencies in different measured properties of the same sample. Roughly speaking: the heat capacity looks characteristically AFM while the behaviour of the magnetization is typical of FM exchange [33].

In detail, while the sign of  $J_x$  changes at  $0.189\text{\AA}^{-2}$  (corresponding to the frustration parameter passing through the value  $r = -0.275$  for which  $\theta = 0$ ), the spin heat capacity continues to be extremely well described by the HTSE for an AFM. As can be seen in Fig. 6, the scaled spin heat capacity data  $c_s/N_2k_B$  when

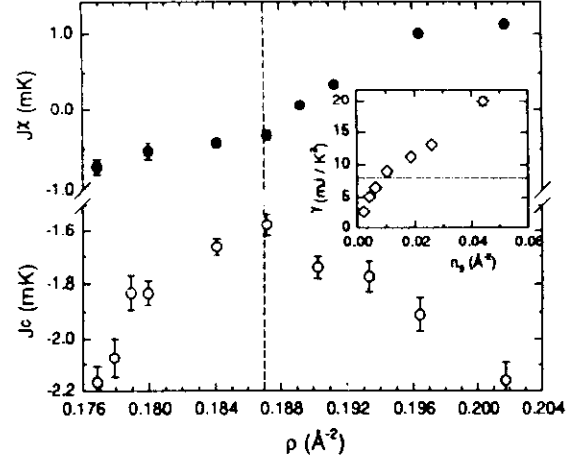


Fig. 5. Coverage dependence of  $J_c$  and  $J_x$ . Vertical dashed line indicates promotion to third layer. Inset: Linear term in heat capacity versus fluid coverage. Dotted line shows Fermi gas result.

plotted against reduced temperature  $T/J_c$  collapse onto a single curve: that expected for a HAFT, over the relatively wide coverage range  $0.178\text{\AA}^{-2}$  to  $0.21\text{\AA}^{-2}$ . Taking an isotherm of the spin heat capacity close to the short range order maximum  $T/J_c = 1$  (Fig. 6 inset) illustrates the constancy of  $c_s/N_2k_B$  at  $0.21$ , as expected for a triangular lattice AFM, up to  $0.21\text{\AA}^{-2}$ . We stress that at  $0.21\text{\AA}^{-2}$  the magnetization data imply a relatively large effective FM exchange constant  $J_x = 1.5\text{mK}$ . At this coverage the frustration parameter is  $-0.19 \pm 0.01$ . Since  $N_2$  is known independently within a few percent, the heat capacity data cannot be explained by models involving the coexistence of AFM and FM regions of the sample [14, 31]. We will discuss these “two-phase”

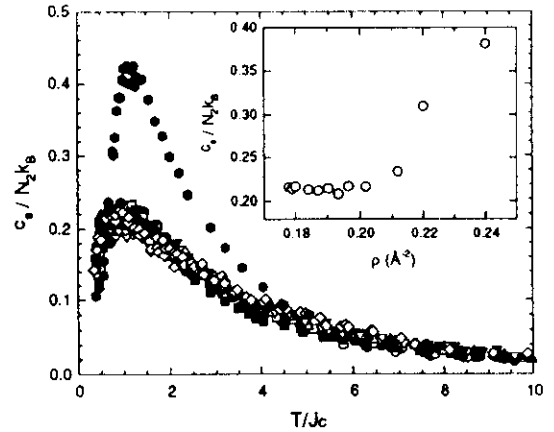


Fig.6. Scaled spin heat capacity for coverages in range  $0.178 - 0.202\text{\AA}^{-2}$ , showing AFM behaviour. Data at FM anomaly are shown for comparison. Inset: Isotherm at  $T/J_c = 1$  to show departure from AFM behaviour near  $0.21\text{\AA}^{-2}$ .

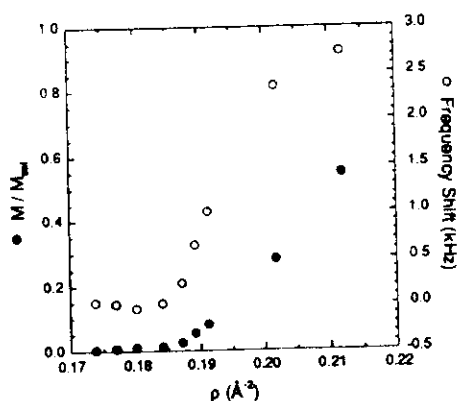


Fig.7. Isotherms of frequency shift and magnetization at 0.8mK, showing onset of significant polarisation.

models further a little later in this section.

This interesting behaviour can be understood as a consequence of frustrated multiple spin exchange. In exact diagonalisation studies of a  $4 \times 4$  spin array [12], the transition from AFM-like to FM-like behaviour occurs at different values of the frustration for heat capacity and magnetization, as observed. Further Roger finds in a mean field calculation [20], that a FM ground state will be stable if  $J_2 - 2J_3 + 4J_4 + 2J_6 < 0$ . This corresponds to  $r > -0.17$ , remarkably close to the frustration ( $r \approx -0.19$ ) at which we find the heat capacity departs from an AFM temperature dependence.

To emphasize this interesting result, there is a parameter range for which the Curie Weiss constant  $\theta$  is positive, as expected for a FM, but the ground state is *not* FM. In the model calculation that parameter range corresponds to  $-0.275 < r < -0.17$ .

This corresponds to coverages from 0.189 to near  $0.21 \text{\AA}^{-2}$ . Exactly what might the ground state be over this coverage range? Although the heat capacity looks AFM, as discussed, the observed spin polarization at the lowest temperatures is large. A magnetization isotherm is shown in Fig. 7 [34]. This has a break at  $0.186 \text{\AA}^{-2}$  shortly before the change in sign of  $J_x$  and close to third layer promotion. Measurements of the frequency shift also show an onset at this coverage and are associated with the dipolar demagnetizing field arising from the large polarization. Similar behaviour was also seen by the Stanford group [31], who in measurements to 80  $\mu\text{K}$  were able to infer the saturation magnetization.

The position of the break in the magnetization isotherm should be contrasted with the break in the heat capacity isotherm (Fig. 6 insert), which does not occur until near  $0.21 \text{\AA}^{-2}$ . Because both magnetization and heat capacity measurements were performed on the

same cell, this result is not subject to uncertainties related to coverage scale.

We propose that these data can be reconciled if the ground state of the system at these coverages is a canted AFM, analogous to the CNAF phase or pseudo-ferromagnetic phase proposed as the "high field phase" for bulk solid  $^3\text{He}$  [7, 9, 28, 36]. Such a state has been suggested in 2D by Roger [20] and is induced by cyclic exchange processes, similar to what is seen theoretically on square lattices. The crucial difference between 2D  $^3\text{He}$  and bulk is that in 2D the frustration can be tuned over a much wider range. This presumably results in a range of frustration for which the canted AFM is the stable zero field phase.

The mean field prediction of the magnetization in zero field is greater than 0.75 of the saturation magnetization for  $r > -0.3$ . This is larger than is observed. Clearly quantum fluctuations have to be included to obtain reliable values. To account for the observed AFM-like heat capacity, we note that a canted AFM would still retain much of the symmetry of the AFM ground state. Thus there are three sub-lattices and the component of the magnetization normal to the field rotates by  $120^\circ$  as in the classical AFM ground state [20]. Detailed calculations of the thermodynamic properties are required.

It is necessary to make a few rather technical comments on the rival "two-phase" models of adsorbed  $^3\text{He}$  films. A second layer phase diagram was proposed by Greywall [14] based on an interpretation of the locus of heat capacity melting peaks of the second layer solid determined by the Seattle group [37]. As the coverage of the film is increased this requires a transformation between two commensurate phases (called R2a and R2b in ref. [14]) and subsequently between the second commensurate phase (R2b) and an incommensurate solid. It was argued [14] that an isotherm of the spin heat capacity at 3mK, linear in second layer density, supported the existence of a coexistence region between R2a and R2b. But we can account quantitatively for our recent heat capacity data over this coverage range simply in terms of a triangular lattice of increasing surface density. A coexistence between an AFM phase and an FM phase was also proposed in ref. [31], to account for the magnetization data. However the heat capacity and magnetization isotherms reported here, taken together, appear not to support a model involving coexisting phases with differing magnetic properties.

In fact the evidence to support the proposed second layer phase diagram from heat capacity "melting" peaks is not strong. What is seen in  $^4\text{He}$  films is that the melting temperature of the second layer solid jumps

down on formation of a fluid overlayer [38], with no clear signature of distinct structural phases. The Seattle data for  $^3\text{He}$  films follow a similar pattern, (with a justifiable coverage scaling of 4% [13]). We note, however, that this data does not conclusively rule out some structural effect at  $0.21\text{\AA}^{-2}$ .

An alternative hypothesis to that of coexisting phases, but drawing on the same database, was to suppose two dimensional condensation of the third layer fluid [39]. In this model the 2D fluid puddles drive regions of the second layer solid beneath them FM. However the present heat capacity measurements find no evidence for this. At third layer densities  $> 0.01\text{\AA}^{-2}$  the coverage dependence of the fluid heat capacity  $\gamma$  is characteristic of a *uniform* weakly interacting Fermi fluid (see Fig. 6 inset). Here the ability to fit the spin contribution for the first time and hence extract that of the fluid overlayer is important.

Finally we note that at coverages  $0.212$  and  $0.22\text{\AA}^{-2}$  the temperature dependence of the spin heat capacity is anomalous. This may suggest the intervention of more exotic ground states between the proposed canted AFM and FM with increasing coverage.

### 5.3 Summary and future prospects

The view expounded here is that the evolving magnetism of the second solid layer of  $^3\text{He}$  can be understood in terms of frustrated multiple spin exchange (MSE) on a triangular lattice, as proposed by Roger [20]. It appears that there is no recourse necessary to models of mixed phases.

One consequence of MSE is that different effective exchange interactions control different thermodynamic properties. Indeed the system may have a magnetization characteristic of FM exchange but a heat capacity that is AFM in character, reflecting an AFM ground state. As emphasised by Roger, a study of the magnetic field dependence should give further confirmation of this picture (although typical fields used in NMR, of order 30mT, have no discernable effect on the heat capacity). On the basis of magnetization and heat capacity data we have suggested a scenario in which tuning the frustration takes the system through a series of ground states  $\text{AFM} \rightarrow \text{canted AFM} \rightarrow ? \rightarrow \text{FM}$ .

Prior to the formation of a fluid overlayer, we are dealing with a genuinely two-dimensional  $S = 1/2$  nuclear antiferromagnet on a triangular lattice. This is potentially an ideal system for the investigation of quantum antiferromagnetism. This is the first system to demonstrate agreement with recently derived HTSE to  $T < J$  for the triangular lattice. Further work is needed to establish the ground state order and to examine the

nature of the spin wave excitations at very low  $T$ .

### 6. Possible phase transition in a 2D antiferromagnet

Very recent measurements on a single monolayer of  $^3\text{He}$  adsorbed on graphite with a bilayer preplating of HD have revealed what may be the signature of a magnetic phase transition. Although this work is at a preliminary stage, we believe the results are of sufficient interest to describe briefly here.

In the previous discussion of pure  $^3\text{He}$  films we have emphasized that the data show no evidence of a phase transition at finite  $T$ . Our motivation to use hydrogen preplated graphite was, in part, to enhance the exchange constants to allow studies to lower  $T/J$ .

Heat capacity isotherms show that the layer first solidifies at  $0.0555\text{\AA}^{-2}$ ; this density is suggestive of a triangular lattice in  $4/7$  commensuration with the HD bilayer, as discussed in Section 2. We may therefore hope to compare the behaviour of this system directly with that of the second layer in pure  $^3\text{He}$  films on first solidification. We find the exchange constants are significantly enhanced relative to the pure  $^3\text{He}$  film. A fit to the heat capacity above 10mK finds  $J_c = -3.7\text{mK}$ , while  $J_\chi = -1.15\text{mK}$ . While these numbers are approximately a factor of two greater than in pure  $^3\text{He}$  films, the ratio  $J_\chi/J_c$  is very close, indicating a similar frustration. The main new feature we observe is a pronounced and relatively sharp heat capacity peak below a broad short range order maximum (Fig. 8). This sharp peak occurs at  $T/J_c \sim 1/3$ . This should encourage a search for a similar feature in pure  $^3\text{He}$  films.

A variety of possibilities suggest themselves: (i) a topological phase transition associated with the appearance of spin vortices [40], (ii) a spin Peierls

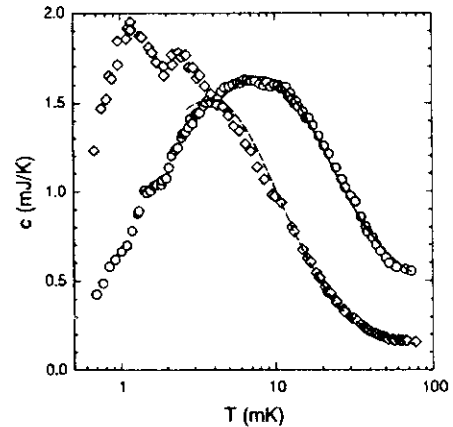


Fig. 8. Heat capacity on graphite plated by a bilayer of HD. Data at  $0.0555\text{\AA}^{-2}$  (●) in solid. Also shown data at  $0.0545\text{\AA}^{-2}$  (○), just inside coexistence region.

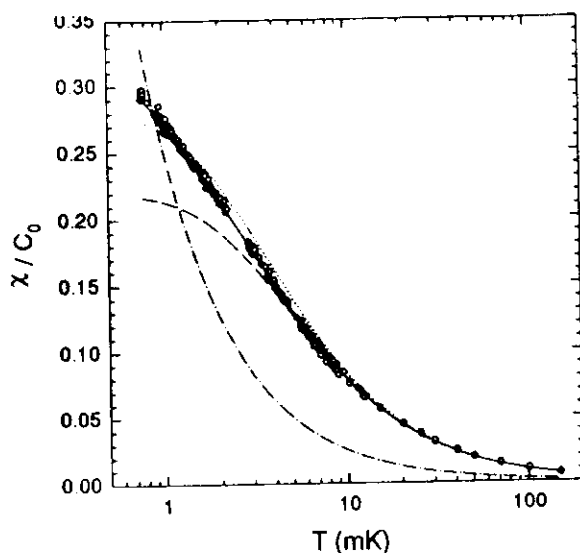


Fig. 9 Magnetization of AFM solid at  $0.0555\text{\AA}^{-2}$ . These are best described by a Curie-Weiss law (solid line). Other lines are (i) best fit to PA for HAFT (dotted) (ii) extrapolation of fit to PA for HAFT for  $T > 10\text{mK}$  (dashed) (iii) magnetization that would arise from 25% free spins (dashed - dotted).

transition [41], (iii) dipolar induced LRMO [42]. We can rule out effects associated with defects in the  $^3\text{He}$  monolayer because there is no marked qualitative change in behaviour between  $0.0555$  and  $0.0565\text{\AA}^{-2}$ , after the film has solidified. The spin-Peierls transition is associated with the formation of singlet dimers. This would result in a sharp decrease in magnetization, which is not observed (Fig. 9). Dipolar induced LRMO is also possible in an FM system, and has been reported in experiments on the  $^3\text{He}$  boundary layer [43], however there is no evidence for it at the FM anomaly in this system. Of course the peak may not arise from a phase transition; MSE calculations for 16 spins find additional peaks in the heat capacity at low  $T$  ascribed to the large density of low lying excitations. However the effect of the finite sample size on these calculations cannot be ruled out; also the peaks found theoretically are broad and occur at significantly lower  $T/J$  than observed.

In fact a large cusp-like peak in the heat capacity coupled with the lack of any pronounced signature in the magnetization is precisely the signature of a topological phase transition found in the classical Heisenberg system. At first sight this seems surprising since the magnetization has three degrees of freedom. However, as pointed out by Kawamura and Miyashita [40], the order parameter of the classical HAFT is a triad of vectors, just like superfluid  $^3\text{He-A}$ . This can sustain topologically stable defects: spin vortices. The

topological transition occurs at the temperature at which the free energy is lowered by populating the system with defects, rather like the Kosterlitz-Thouless superfluid transition of 2D  $^4\text{He}$ . Computer simulations find a cusp in the heat capacity and a jump in the spin correlation length at  $T_c$  [40, 44]. Note that above and below  $T_c$  this correlation length diverges exponentially with decreasing temperature. There is no long range order in the spin system. Defining a vorticity function which essentially measures the twist in the spin system round a closed contour, and considering a circular contour centred on the vortex core, then for  $T > T_c$  the vorticity decays exponentially with the area of the circle, while for  $T < T_c$  it decays as the circle's perimeter [40]. To the extent that the quantum spin system has a  $T = 0$  order with the same symmetry as the classical spin system, then it is plausible that a similar transition could occur in the  $S = 1/2$  case.

An interesting feature of the magnetization is that it follows a Curie Weiss law (surprisingly to  $T/\theta \sim 0.25$ ) much better than the Padé approximant to the HTSE for a HAFT (Fig. 9) [45]. Such behaviour is believed to be characteristic of strong frustration and has been seen in other quasi-two dimensional magnetic systems [46]. These effects are much easier to discern on preplated substrates than in pure  $^3\text{He}$  films due to the absence of the paramagnetic first layer. Hopefully the present results will motivate MSE calculations of the susceptibility. The contribution of 25% free spins is also shown in the figure; this shows that the model of the commensurate triangular lattice as a *kagomé* net plus 25% free spins cannot be sustained.

Much more work is needed to characterise this system, through a full study of the coverage dependance of magnetization and heat capacity.

## Conclusion

We have tried to emphasize the potential importance of 2D solid  $^3\text{He}$  as a model for the experimental study of quantum antiferromagnetism and frustrated cyclic spin exchange. The possibility to access a range of different ground states by tuning the frustration is particularly intriguing, and we have provided experimental evidence for this. There is a real need for further theory to explore the  $T = 0$  and finite temperature properties of these systems.

## Acknowledgements

It is a pleasure to thank B. Bernu, D. Ceperley, J. Chalker, N. Elstner, M. Long and M. Roger for stimulating discussions and correspondence. This work was supported by EPSRC (U.K.)

## References

- [1] A. P. Ramirez, these proceedings
- [2] D. A. Huse and V. Elser, Phys. Rev. Lett. 60, 2531 (1988), B. Bernu, C. Lhuillier and L. Pierre, Phys. Rev. Lett. 69, 2590 (1992), T. Jolicoeur and J. C. Le Guillou, Phys. Rev. B40, 2727 (1989)
- [3] see P. W. Leung and Ngar-Wing Lam, Phys. Rev. B53, 2213 (1996) and refs. therein. A. Chubukov, E. Gagliano and C. Balseiro, Phys. Rev. B45, 7889 (1992)
- [4] K. Hirakawa, H. Kadowaki and K. Ubukoshi, J. Phys. Soc. Jap. 54, 3526 (1985)
- [5] S. T. Bramwell *et al.* J. Phys. CM. 8, L123 (1996)
- [6] D. J. Thouless, Proc. Phys. Soc. London 86, 893 (1965)
- [7] M. Roger, J. H. Hetherington and J. M. Delrieu, Rev. Mod. Phys. 55, 1 (1983)
- [8] K. K. Nummila, these proceedings
- [9] M. Cross, Jap. Journ. App. Phys. 26, 1855 (1987)
- [10] D. M. Ceperley, Rev. Mod. Phys. 67, 279 (1995)
- [11] D. M. Ceperley and G. Jacucci, Phys. Rev. Lett. 58, 1648 (1988)
- [12] B. Bernu, D. M. Ceperley and C. Lhuillier, J. Low Temp. Phys. 89, 589 (1992)
- [13] The structural and magnetic properties of  $^3\text{He}$  films on graphite are reviewed in: H. Godfrin and H. -J. Lauter, Prog. Low Temp. Phys. XIV, 213 (1995) and H. Godfrin and R. E. Rapp, Adv. Phys. 44, 113 (1995)
- [14] D. S. Greywall, Phys. Rev. B41, 1842 (1990), Physica B197, 1 (1994) and references therein.
- [15] V. Elser, Phys. Rev. Lett. 62, 2405 (1989)
- [16] M. Siqueira, C. P. Lusher, B. P. Cowan and J. Saunders, Phys. Rev. Lett. 71, 1407 (1993)
- [17] O. E. Vilches, R. C. Ramos Jr., D. A. Ritter, these proceedings.
- [18] F. F. Abraham, J. Q. Broughton, P. W. Leung and V. Elser, Europhys. Lett. 12, 107 (1990)
- [19] C. P. Lusher, J. Saunders and B. P. Cowan, Europhys. Lett. 14, 809 (1990)
- [20] M. Roger, Phys. Rev. Lett. 64, 297 (1990)
- [21] M. Siqueira, J. Nyéki, B. Cowan and J. Saunders, Phys. Rev. Lett. 76, 1884 (1996)
- [22] N. Elstner, R. R. P. Singh and A. P. Young, Phys. Rev. Lett. 71, 1629 (1993)
- [23] D. S. Greywall and P. A. Busch, Physica 65 & 166B, 23 (1990)
- [24] N. Elstner and A. P. Young, Phys. Rev. B50, 6871 (1994)
- [25] M. Siqueira, J. Nyéki, B. P. Cowan and J. Saunders, J. Low Temp. Phys. 101, 713 (1995)
- [26] H. Godfrin *et al.* Physica 194-196B, 675 (1994)
- [27] C. Bäuerle, Yu. M. Bunkov, S. N. Fisher and H. Godfrin, these proceedings.
- [28] discussed by M. C. Cross and D. S. Fisher, Rev. Mod. Phys. 57, 881 (1985) and ref. [10].
- [29] H. Franco, R. E. Rapp and H. Godfrin, Phys. Rev. Lett. 1161 (1986); H. Godfrin, R. E. Rapp and H. -J. Lauter, Physica B169, 177 (1991); see also ref. [13].
- [30] H. Godfrin, R. R. Ruel and D. D. Osheroff, Phys. Rev. Lett. 60, 305 (1988)
- [31] P. Schiffer, M. T. O'Keefe, D. D. Osheroff and H. Fukuyama, Phys. Rev. Lett. 71, 1403 (1993) and J. Low Temp. Phys. 94, 489 (1994)
- [32] C. Bäuerle *et al.*, J. Low Temp. Phys. 101, 457 (1995) and these proceedings.
- [33] M. Siqueira *et al.*, these proceedings
- [34] M. Siqueira, J. Nyéki, C. P. Lusher, B. P. Cowan and J. Saunders, Phys. Rev. B50, 13069 (1994); the coverages have been scaled for consistency.
- [36] H. Godfrin and D. D. Osheroff, Phys. Rev. B38, 4492 (1988); see also recent review by D. D. Osheroff, J. Low Temp. Phys. 87, 297 (1992)
- [37] S. W. Van Sciver and O. E. Vilches, Phys. Rev. B18, 285 (1978), S. W. Van Sciver, Phys. Rev. B18, 277 (1978)
- [38] D. S. Greywall, Phys. Rev. B47, 309 (1993)
- [39] H. Godfrin, R. E. Rapp, K. -D. Morhard, J. Bossy and C. Bäuerle, Phys. Rev. B49, 12377 (1994)
- [40] H. Kawamura and S. Miyashita, J. Phys. Soc. Jap. 53, 4138 (1984)
- [41] J. B. Marston and C. Zeng, J. App. Phys. 69, 5962 (1991)
- [42] C. Pich and F. Schwabl, Phys. Rev. B47, 7957 (1993)
- [43] L. J. Friedman, A. L. Thomson, C. M. Gould, H. M. Bozler, P. B. Weichman and M. C. Cross, Phys. Rev. Lett. 62, 1635 (1989)
- [44] M. Wintel, H. U. Everts and W. Apel, Europhys. Lett. 25, 711 (1994)
- [45] In previous experiments on this system, ref. [16], larger values of  $\theta$  were reported. We believe these arose from non-uniformities in the preplating that occurred due to a cell with a relatively large dead volume.
- [46] A. P. Ramirez, G. P. Espinosa and A. S. Cooper, Phys. Rev. Lett. 2070 (1990)

